

1998

Reactions of 10-methyl-9,10-dihydroacridine with inorganic oxidants

Oleg E. Pestovsky
Iowa State University

Follow this and additional works at: <https://lib.dr.iastate.edu/rtd>

 Part of the [Inorganic Chemistry Commons](#)

Recommended Citation

Pestovsky, Oleg E., "Reactions of 10-methyl-9,10-dihydroacridine with inorganic oxidants " (1998). *Retrospective Theses and Dissertations*. 11881.
<https://lib.dr.iastate.edu/rtd/11881>

This Dissertation is brought to you for free and open access by the Iowa State University Capstones, Theses and Dissertations at Iowa State University Digital Repository. It has been accepted for inclusion in Retrospective Theses and Dissertations by an authorized administrator of Iowa State University Digital Repository. For more information, please contact digirep@iastate.edu.

INFORMATION TO USERS

This manuscript has been reproduced from the microfilm master. UMI films the text directly from the original or copy submitted. Thus, some thesis and dissertation copies are in typewriter face, while others may be from any type of computer printer.

The quality of this reproduction is dependent upon the quality of the copy submitted. Broken or indistinct print, colored or poor quality illustrations and photographs, print bleedthrough, substandard margins, and improper alignment can adversely affect reproduction.

In the unlikely event that the author did not send UMI a complete manuscript and there are missing pages, these will be noted. Also, if unauthorized copyright material had to be removed, a note will indicate the deletion.

Oversize materials (e.g., maps, drawings, charts) are reproduced by sectioning the original, beginning at the upper left-hand corner and continuing from left to right in equal sections with small overlaps. Each original is also photographed in one exposure and is included in reduced form at the back of the book.

Photographs included in the original manuscript have been reproduced xerographically in this copy. Higher quality 6" x 9" black and white photographic prints are available for any photographs or illustrations appearing in this copy for an additional charge. Contact UMI directly to order.

UMI

A Bell & Howell Information Company
300 North Zeeb Road, Ann Arbor MI 48106-1346 USA
313/761-4700 800/521-0600

Reactions of 10-methyl-9,10-dihydroacridine with inorganic oxidants

by

Oleg E. Pestovsky

A dissertation submitted to the graduate faculty
in partial fulfillment of the requirements for the degree of
DOCTOR OF PHILOSOPHY

Major: Inorganic Chemistry
Major Professor: James H. Espenson

Iowa State University

Ames, Iowa

1998

UMI Number: 9841076

**UMI Microform 9841076
Copyright 1998, by UMI Company. All rights reserved.**

**This microform edition is protected against unauthorized
copying under Title 17, United States Code.**

UMI
300 North Zeeb Road
Ann Arbor, MI 48103

**Graduate College
Iowa State University**

**This is to certify that the doctoral dissertation of
Oleg E. Pestovsky
has met the dissertation requirements of Iowa State University**

Signature was redacted for privacy.

Major Professor

Signature was redacted for privacy.

For the Major Program

Signature was redacted for privacy.

For the Graduate College

TABLE OF CONTENTS

	<u>Page</u>
GENERAL INTRODUCTION	1
Introduction	1
Dissertation Organization	5
References	6
CHAPTER I. REACTIONS OF 10-METHYL-9,10-DIHYDROACRIDINE WITH INORGANIC OXIDIZING REAGENTS IN ACETONITRILE/WATER MIXED SOLVENT: A UNIFIED VIEW ON OXIDATION OF DIHYDROACRIDINE	9
Abstract	9
Introduction	10
Experimental Section	11
Materials	11
Kinetic studies	12
Cyclic voltammetry	13
Results	13
Reaction with Ce(IV)	13
Kinetic isotope effects in Ce(IV) reactions	18
Reaction with hexachloroiridate(IV)	21
Reaction with aqueous iron(III)	22

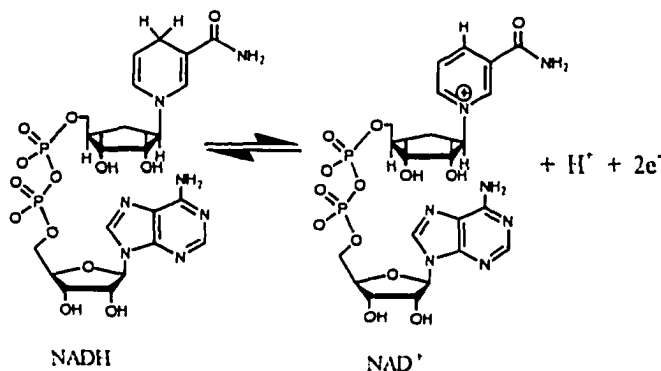
Cyclic voltammetry of AcrH ₂ in AN and AN/H ₂ O mixed solvents	23
Discussion	23
The reaction of dihydroacridine with Ce(IV)	23
The reaction of dihydroacridine with IrCl ₆ ²⁻	30
Reaction with iron(III)	31
General mechanism of one-electron oxidation of dihydroacridine	32
Acknowledgement	33
References	33
CHAPTER II. REACTIONS OF 10-METHYL-9,10-DIHYDROACRIDINE WITH CHROMATE	38
Abstract	38
Introduction	39
Experimental Section	40
Materials	40
Kinetic studies and instrumentation	41
Results	42
Stoichiometry of the reaction between AcrH ₂ and chromate	42
Kinetics of the reaction between AcrH ₂ and chromate in oxygen-and air-saturated solutions	45
Kinetics of the reaction between AcrH ₂ and chromate under air-free conditions	52
Kinetic isotope effect studies	54
Reaction of chromyl ion (CrO ²⁺) with AcrH ₂	60

Discussion	61
General observations and the reaction scheme	61
The initiation step in the chain reaction	67
The role of superoxochromim(III)	68
Reactions of AcrH_2 with hydrogen chromate vs. dichromate in the chain reaction	70
Reactions of AcrH_2 with Cr^{V} Intermediates	71
Reaction of AcrH_2 with excess chromate under anaerobic conditions	72
Acid effect on the reaction between AcrH_2 and excess chromate under anaerobic conditions	75
Conclusions	76
Acknowledgement	77
References	77
GENERAL CONCLUSIONS	82
ACKNOWLEDGEMENTS	84

GENERAL INTRODUCTION

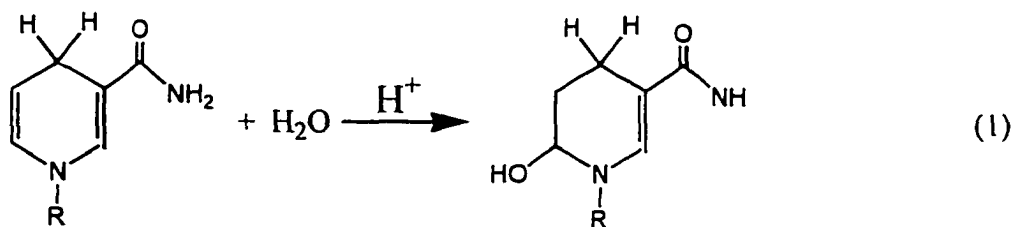
Introduction

Dihydropyridines and their substituted analogs have attracted considerable attention due to their importance as dihydronicotinamide dinucleotide (NADH) models in biological redox reactions.¹⁻⁴



References 1 through 4 correspond to the NADH studies, NADH modeling studies, free radicals and radical-cations of dihydropyridine analogs and their properties, and nonradical chemistry of dihydropyridines, respectively.

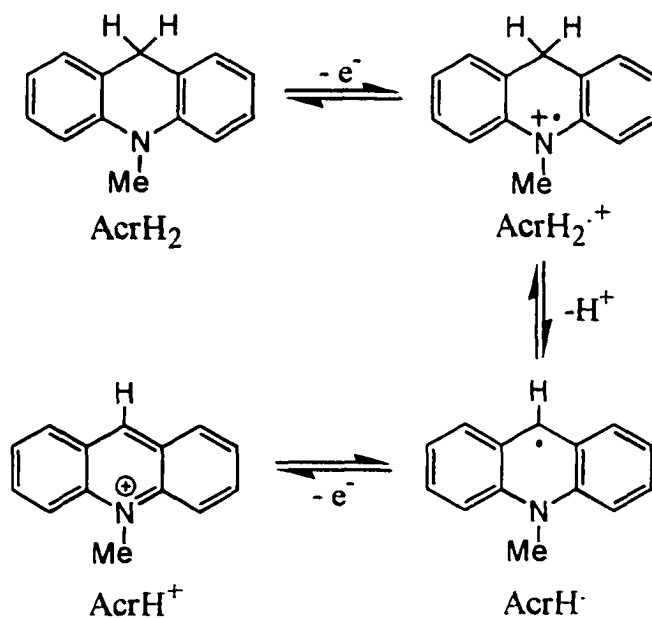
In particular, 10-methyl-9,10-dihydroacridine (AcrH₂) has been successfully employed in mechanistic studies of its reactions with various organic and inorganic oxidizing reagents.⁵ The unique stability of dihydroacridines towards acid-catalyzed hydrolysis⁶ (eq 1) has allowed extensive kinetic studies of their reactions with strong inorganic oxidants that often require acidic media.



Hydride transfer, hydrogen atom abstraction, and electron transfer mechanisms have been proposed for oxidation of AcrH₂ by various organic and inorganic reagents. Hydride transfer was found in self-exchange reactions between dihydropyridine analogs and corresponding pyridinium cations. Similar mechanism was observed in oxidation of AcrH₂ by ketones and other carbonyl-containing compounds (Kreevoy, 1983). Hydrogen atom abstraction mechanism was reported for oxidation of AcrH₂ by oxygen and alkyl or aryl halides (Fukuzumi, 1983). Electron transfer oxidation of AcrH₂ was recently reported in the reactions with Cu²⁺, Fe(phen)₃³⁺, and Fe³⁺ in acetonitrile (Saveant, 1990; Fukuzumi, 1993).

Electrochemical properties of AcrH₂ are also well known from recent studies by Saveant and Fukuzumi. Scheme I shows electrochemical reactions of AcrH₂ in acetonitrile.

Scheme I

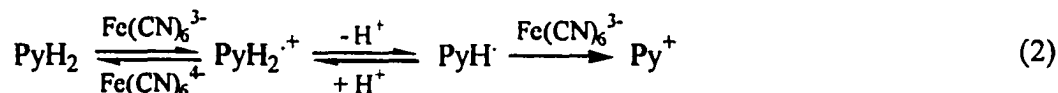


$$E^0 (\text{AcrH}_2^{\bullet+}/\text{AcrH}_2) = 1.02 \text{ V (vs. NHE)}$$

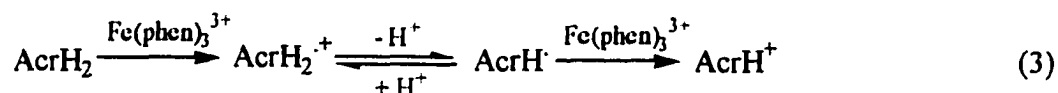
$$E^0 (\text{AcrH}^+/\text{AcrH}^{\bullet}) = -0.19 \text{ V (vs. NHE)}$$

$$pK_a (\text{AcrH}_2^{\bullet+}) = 7.8 \text{ (Fukuzumi)}, 0.6 \text{ (Saveant)}$$

Bruice et al.⁷ have reported a kinetic study of the oxidation of dihydropyridines by ferricyanide to the corresponding pyridinium cations in two consecutive one-electron steps, with the first step being rate controlling, eq 2.



Recently, a similar mechanism for oxidation of AcrH₂ by tris-phenanthroline iron(III) complex in acetonitrile (AN) has been proposed by Fukuzumi et al.,⁸ eq 3.



In this mechanism, the deprotonation of the radical cation is rate-controlling. The dihydropyridine radical cation was identified and characterized by UV-VIS and ESR spectroscopy. The pK_a of the radical cation was also determined.

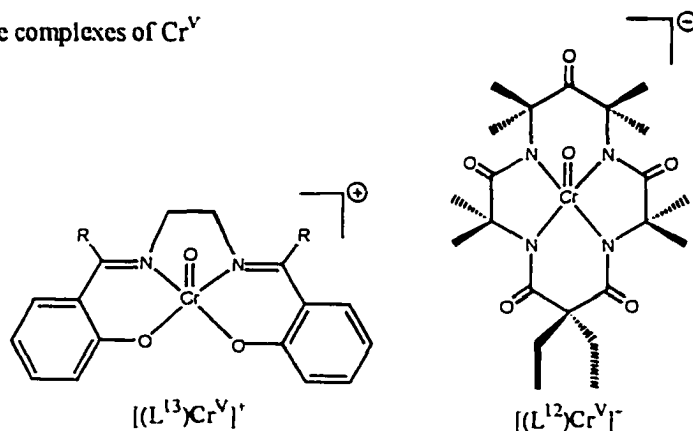
Several factors, such as the oxidizing strength of the reagents used or the medium, can be responsible for the change in the rate-controlling step from the initial electron transfer to the deprotonation of the radical cation. It is still unknown which factors are most important. A further mechanistic study utilizing a systematic change in these factors should provide necessary information to answer this question.

Although the mechanism of AcrH₂ oxidation in non-aqueous solvents now seems to be well understood, little is known about the kinetic behavior of dihydroacridines in semi-aqueous and aqueous media. More experimental data for these types of AcrH₂ reactions are necessary, especially considering the biological importance of aqueous chemistry. In this study we employed several inorganic oxidizing reagents to devise a unified mechanistic picture of AcrH₂ oxidation in AN/H₂O mixed solvent. The reduction

potential of the inorganic oxidants was varied over a wide range to cover different modes of the oxidation mechanism. It can be shown that all the mechanisms fit into one scheme, where the strength of the oxidant determines which mode of oxidation the reaction adopts. The properties of AcrH_2 and its radical cation, such as the pK_a values and one-electron oxidation potentials, can also be determined in this medium, the most interesting being the H/D kinetic isotope effect for the acid ionization of the dihydroacridine radical cation.

Dihydroacridine has proven to be an excellent kinetic probe for monitoring Cr(IV) and Cr(V) species which are proposed to be important intermediates in various organic oxidations with chromate. Although aqua chromyl(IV) (CrO^{2+}) has been characterized in terms of its properties and reactivity,⁹ the instability of the Cr(V) intermediates derived from chromate has precluded the direct determination of their properties. The transient complex $\text{trans}-(\text{H}_2\text{O})\text{LCrO}^{3+}$ ($\text{L}=[14]\text{aneN}_4$) undergoes one-electron oxidation reactions with various organic and inorganic reducing reagents.¹⁰ Several other stable Cr(V) complexes employing chelating and macrocyclic ligands to stabilize this unusual oxidation state have been reported.¹¹

Some stable complexes of Cr^{V}



Since mechanistic or kinetic data are not available for the redox reactions of Cr(V) intermediates derived from simple chromate, it is desirable to obtain more data concerning the fundamental properties and reactivity of such species.

Here we propose a detailed mechanism for the reaction between 9-methyl-9,10-dihydroacridine and chromate ions in a mixed acetonitrile-water solvent. By applying conventional UV-VIS spectrophotometry and stopped-flow techniques, Cr(IV) and Cr(V) species could be identified as important intermediates in this system. From the implications of the chain-reaction mechanism found to operate in this system in the absence of oxygen, we have been able to determine the reactivities of Cr(IV) and Cr(V) intermediates in competitive electron transfer, hydrogen atom abstraction, and hydride transfer. Also to be noted is a specific inhibiting effect of oxygen which is different from the effect reported by Bruice et al.⁷ in the oxidation of dihydropyridines with ferricyanide, which arises from the reaction between pyridinium radicals and O₂.

Dissertation Organization

The dissertation consists of two chapters. Chapter I corresponds to a paper published in *Inorganic Chemistry*. Chapter II is a manuscript to be submitted to the *Journal of the American Chemical Society*. Each chapter is self-contained with its own equations, figures, tables, schemes and references. Following the last manuscript is general conclusions. With the exception for the cyclic voltammetry measurements (Chapter I) which were performed by Dr. Victor Adamian, all the work in this dissertation was performed by the author of this thesis, Oleg E. Pestovsky.

References

- (1) (a) Eisner, U.; Kuthan, J. *Chem. Rev.* **1972**, *72*, 1. (b) Stout, D. M.; Mayer, A. I. *Ibid.* **1982**, *82*, 223. (c) Shinkai, S.; Bruice, T. *Biochemistry* **1973**, *12*, 1750. (d) Kurz, L.; Frieden, C. *J. Am. Chem. Soc.* **1975**, *97*, 667. (e) Jones, J.; Taylor, K. *Can. J. Chem.* **1976**, *54*, 2974.
- (2) (a) Ohnishi, Y.; Ohno, A. *Chem. Lett.* **1976**, 697. (b) Kill, R.; Widdowson, D. J. *Chem. Soc., Chem. Commun.* **1976**, 697. (c) van Eikeren, P.; Grier, D. *J. Am. Chem. Soc.* **1977**, *99*, 8057. (d) Hajdu, J.; Sigman, D. *Ibid.* **1976**, *98*, 6060. (e) Schmakel, C.; Santhanathan, K.; Elving, P. *J. Electrochem. Soc.* **1974**, *121*, 345.
- (3) (a) Kosower, E. M. In *Free Radicals in Biology*; Pryor, W. A., Ed.; Academic Press: New York, 1976; Vol. II, p 1. (b) Kill, R. J.; Widdowson, D. A. In *Bioorganic Chemistry*; van Tamelen, E. E., Ed.; Academic Press: New York, 1978; Vol. IV, p 239. (c) Bruice, T. C. In *Progress in Bioinorganic Chemistry*; Kaiser, F. T., Kezdy, F. J., Eds.; Wiley: New York, 1976; Vol. IV, p 1. (d) Yasui, S.; Ohno, A. *Bioorg. Chem.* **1986**, *14*, 70.
- (4) (a) Roberts, R. M. G.; Ostovic, D.; Kreevoy, M. M. *J. Org. Chem.* **1983**, *48*, 2053. (b) Blaedel, W. J.; Haas, R. G. *Anal. Chem.* **1970**, *42*, 918. (c) Sinha, A.; Bruice, T. C. *J. Am. Chem. Soc.* **1984**, *106*, 7291. (d) Fukuzumi, S.; Hironaka, K.; Tanaka, T. *Ibid.* **1983**, *105*, 4722.
- (5) (a) Fukuzumi, S. In *Advances in Electron Transfer Chemistry*; Mariano, P. S., Ed.; JAI Press: Greenwich, 1992; Vol. 2, p 65. (b) van Eikeren, P.; Grier, D. L. *J. Am. Chem. Soc.* **1976**, *98*, 4655. (c) Fukuzumi, S.; Kuroda, S.; Goto, T.; Ishikawa, K.; Tanaka, T. *J. Chem. Soc., Perkin Trans. II* **1989**, 1047. (d) Fukuzumi, S.; Ishikawa,

- M.; Tanaka, T. *J. Chem. Soc., Perkin Trans.* **1989**, 1037. (e) Ishikawa, K.; Fukuzumi, S.; Goto, T.; Tanaka, T. *J. Am. Chem. Soc.* **1990**, *112*, 1577. (f) Fukuzumi, S.; Chiba, M.; Tanaka, T. *Chem. Lett.* **1989**, 31. (g) Fukuzumi, S.; Mochizuki, S.; Tanaka, T. *J. Am. Chem. Soc.* **1989**, *111*, 1497. (h) Fukuzumi, S.; Mochizuki, S.; Tanaka, T. *Inorg. Chem.* **1990**, *29*, 653. (i) Fukuzumi, S.; Tokuda, Y. *J. Phys. Chem.* **1993**, *97*, 3737.
- (6) (a) van Eikeren, P.; Grier, D. L.; Eliason, J. *J. Am. Chem. Soc.* **1979**, *101*, 7406. (b) Kim, C. S. Y.; Chaykin, S. *Biochemistry* **1968**, *7*, 2339. (c) Fukuzumi, S.; Ishikawa, M.; Tanaka, T. *Tetrahedron* **1986**, *42*, 1021.
- (7) Powell, M. F.; Wu, J. G.; Bruice, T. C. *J. Am. Chem. Soc.* **1984**, *106*, 3850.
- (8) Fukuzumi, S.; Tokuda, Y.; Kitano, T.; Okamoto, T.; Otera, J. *J. Am. Chem. Soc.* **1993**, *115*, 8960.
- (9) (a) Scott, S. L.; Bakac, A.; Espenson, J. H. *J. Am. Chem. Soc.* **1992**, *114*, 4205 (b) Al-Ajlouni, A. M.; Espenson, J. H.; Bakac, A. *Inorg. Chem.* **1993**, *32*, 3162 (c) Brynildson, M. E.; Bakac, A.; Espenson, J. H. *Inorg. Chem.* **1988**, *27*, 2592 (d) Ilan, Y. A.; Czapski, G.; Ardon, M. *Isr. J. Chem.* **1975**, *13*, 15 (e) Sellers, R. M.; Simic, M. G. *J. Am. Chem. Soc.* **1976**, *98*, 6145.
- (10) Bakac, A.; Wang, W.-D. *J. Am. Chem. Soc.* **1996**, *118*, 10325.
- (11) (a) Krumpolc, M.; Rocek, J. *J. Am. Chem. Soc.* **1979**, *101*, 3206 (b) Srinivasan, K.; Kochi, J. K. *Inorg. Chem.* **1985**, *24*, 4670 (c) Ghosh, M. C.; Gould, E. S. *J. Am. Chem. Soc.* **1993**, *115*, 3167 (d) Sugden, K. D.; Wetterhahn, K. E. *Inorg. Chem.* **1996**, *35*, 651 (e) Collins, T. J.; Slebodnick, C.; Uffelman, E. S. *Inorg. Chem.* **1990**, *29*, 3433 (f) Siddall, T. L.; Miyaura, N.; Huffman, J. C.; Kochi, J. K. *J. Chem. Soc. Chem. Commun.* **1983**, 1185 (g) Yuan, L.-C.; Bruice, T. C. *J. Am. Chem. Soc.* **1985**,
-

107, 512 (h) Mitewa, M.; Russev, P.; Bontchev, P. R.; Kabassanov, K.; Malinovski, A. *Inorg. Chim. Acta* **1983**, *70*, 179 (i) Gould, E. S. *Acc. Chem. Res.* **1986**, *19*, 66 (j) Bakac, A. *Progress in Inorganic Chemistry*; Karlin, K. D., Ed.; Wiley: New York, 1995; Vol. 43, p 267.

CHAPTER I

**REACTIONS OF 10-METHYL-9,10-DIHYDROACRIDINE WITH
INORGANIC OXIDIZING REAGENTS IN
ACETONITRILE/WATER MIXED SOLVENT:
A UNIFIED VIEW ON OXIDATION OF DIHYDROACRIDINE**

Based on a paper published in *Inorganic Chemistry**

Oleg Pestovsky, Andreja Bakac and James H. Espenson

Abstract

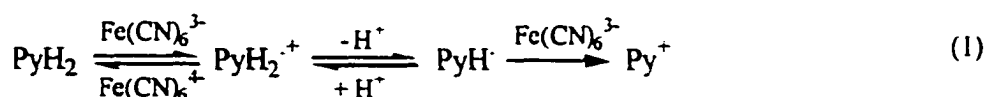
Reactions of 10-methyl-9,10-dihydroacridine with various inorganic oxidants in 20% acetonitrile/80% water solvent mixture fall into two categories depending on the strength of the oxidant used. Rapid electron transfer to the strong oxidizing reagents, Ce^{IV} and IrCl_6^{2-} , produces dihydroacridine radical cations, $\text{AcrH}_2^{+\cdot}$ (λ_{max} 650 nm). This is followed by the rate-determining loss of a proton and rapid oxidation of thus formed AcrH^{\cdot} by the second equivalent of Ce^{IV} or IrCl_6^{2-} . The protonation of AcrH^{\cdot} and deprotonation of $\text{AcrH}_2^{+\cdot}$ exhibit significant kinetic isotope effects. The use of d_2 -acridine in $\text{H}_2\text{O}/\text{CH}_3\text{CN}$ yields the secondary and solvent isotope effects separately. A large normal secondary isotope effect of 1.86 ± 0.17 for the protonation^{*} of the acridinium radical suggests a possibility of nuclear tunneling. The reaction of

* Pestovsky, O.; Bakac, A.; Espenson, J. H. *Inorg. Chem.* 1998, 37, 1616

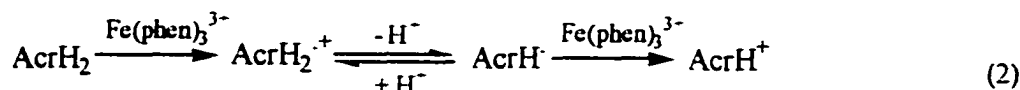
dihydroacridine with a mild oxidizing reagent, Fe^{3+} , is slow and shows no kinetic isotope effect. The initial electron transfer from AcrH_2 to Fe^{3+} is believed to be rate-determining.

Introduction

Dihydropyridines and their substituted analogs have attracted considerable attention due to their importance as dihydronicotinamide dinucleotide (NADH) models in biological redox reactions.¹⁻⁴ In particular, 10-methyl-9,10-dihydroacridine (AcrH_2) has been successfully employed in mechanistic studies of its reactions with various organic and inorganic oxidizing reagents.⁵ The unique stability of dihydroacridines towards acid-catalyzed hydrolysis⁶ has allowed extensive kinetic studies of their reactions with strong inorganic oxidants that often require acidic media. Bruice et al.⁷ have reported a kinetic study of the oxidation of dihydropyridines by ferricyanide to the corresponding pyridinium cations in two consecutive one-electron steps, with the first step being rate controlling, eq 1.



Recently, a similar mechanism for oxidation of AcrH_2 by tris-phenanthroline iron(III) complex in acetonitrile (AN) has been proposed by Fukuzumi et al.,⁸ eq 2.



In this mechanism, the deprotonation of the radical cation is rate-controlling. The dihydroacridine radical cation was identified and characterized by UV-VIS and ESR

spectroscopy. The pK_a of the radical cation was also determined. Several factors, such as the oxidizing strength of the reagents used or the medium, can be responsible for the change in the rate-controlling step from the initial electron transfer to the deprotonation of the radical cation. It is still unknown which factors are most important. A further mechanistic study utilizing a systematic change in these factors should provide necessary information to answer this question.

Although the mechanism of $AcrH_2$ oxidation in non-aqueous solvents now seems to be well understood, little is known about the kinetic behavior of dihydroacridines in semi-aqueous and aqueous media. More experimental data for these types of $AcrH_2$ reactions are necessary, especially considering the biological importance of aqueous chemistry. In this study we employed several inorganic oxidizing reagents to devise a unified mechanistic picture of $AcrH_2$ oxidation in AN/ H_2O mixed solvent. The reduction potential of the inorganic oxidants was varied over a wide range to cover different modes of the oxidation mechanism. It can be shown that all the mechanisms fit into one scheme, where the strength of the oxidant determines which mode of oxidation the reaction adopts. The properties of $AcrH_2$ and its radical cation, such as the pK_a values and one-electron oxidation potentials, can also be determined in this medium, the most interesting being the H/D kinetic isotope effect for the acid ionization of the dihydroacridine radical cation.

Experimental Section

Materials. Perchloric acid (Fisher), acetonitrile (Fisher), deuterium oxide (Aldrich), methyl iodide (Aldrich), ceric(IV) ammonium nitrate (GFS), ammonium

hexachloroiridate(IV) (Aldrich), lithium alumohydride (Aldrich), lithium alumodeuteride (Aldrich), 10-methylacridone (Aldrich), acridine (Aldrich) and iron(III) perchlorate (Aldrich) were used as received. High purity water was obtained by passing laboratory-distilled water through Millipore-Q purification system. Lithium perchlorate was obtained from Aldrich and was recrystallized from water 3 times. 10-methyl-9,10-dihydroacridine (AcrH₂) and its dideuterated analog AcrD₂ were prepared by reduction of 10-methylacridone with LiAlH₄ or LiAlD₄, respectively, according to the literature procedure.⁹ 10-methylacridinium iodide was prepared by the reaction of acridine with methyl iodide according to a standard procedure.¹⁰ The purity of the organic starting materials was checked by ¹H-NMR spectroscopy.

Kinetic studies. All the kinetic studies were carried out in 20% AN / 80% H₂O solvent mixture. All spectroscopic UV-VIS experiments were performed with use of a Shimadzu UV-3101 PC instrument at ambient temperature. Kinetic measurements for AcrH₂/Ce(IV) and AcrH₂/IrCl₆²⁻ reactions were performed with an Applied Photophysics stopped-flow apparatus under anaerobic conditions. The temperature was controlled at 25.0±0.2 °C. Concentrations of AcrH₂ stock solutions were determined spectrophotometrically, $\epsilon_{285}=13,200 \text{ L mol}^{-1} \text{ cm}^{-1}$. The ionic strength of the reaction solutions was maintained at 1 M by addition of lithium perchlorate. Reactions of AcrH₂ and AcrD₂ with Ce(IV) were monitored at 358 nm by observing the formation of acridinium ion ($\epsilon_{358} = 18,800 \text{ L mol}^{-1} \text{ cm}^{-1}$), unless noted otherwise. Stock solutions of IrCl₆²⁻ were standardized spectrophotometrically, $\epsilon_{487}=4075 \text{ L mol}^{-1} \text{ cm}^{-1}$.¹¹ Aqueous solutions of iron(II) were prepared by reduction of iron(III) perchlorate with zinc

amalgam under anaerobic conditions in aqueous 0.1 M HClO₄. The concentration of Fe³⁺ was determined spectrophotometrically, $\epsilon_{240}=4160 \text{ L mol}^{-1} \text{ cm}^{-1}$.¹² Kinetics data were analyzed using Kaleidagraph v3.08 for PC software package. FitSim simulations were performed by converting the absorbance readings to concentration of the product AcrH⁺ using the extinction coefficient difference of the slowest trace as a reference. The fitting was carried out on a Dell XPSPro computer using FitSim v4.0 for PC. For each mechanism, all the experimental traces were fitted simultaneously.

Cyclic voltammetry experiments were carried out with use of a BAS-100 electrochemical analyzer and a three-electrode system consisting of a glassy carbon or platinum disk working electrode, a platinum wire counter electrode and a saturated calomel electrode (SCE) as the reference. The SCE was separated from the bulk of the solution by a low porosity fritted-glass bridge, which contained the solvent/supporting electrolyte mixture. t-Bu₄NPF₆ and NaClO₄ were used as supporting electrolytes in AN and AN/H₂O solvents, respectively.

Results

Reaction with Ce(IV). At a low ceric ion concentration (0.2 mM), the reactions followed first order kinetics in both AcrH₂ and Ce^{IV} concentrations. Identical kinetics were obtained at the absorption maxima for AcrH⁺ (λ_{max} 358 nm and 417 nm) and AcrH₂⁺⁺ (λ_{max} 650 nm). **Figure 1** shows representative traces at 358 nm and 640 nm. The second-order rate constants increase with increasing acid concentration in a nonlinear fashion, as shown in **Figure 2**. A tentative mechanism is shown in **Scheme I**.

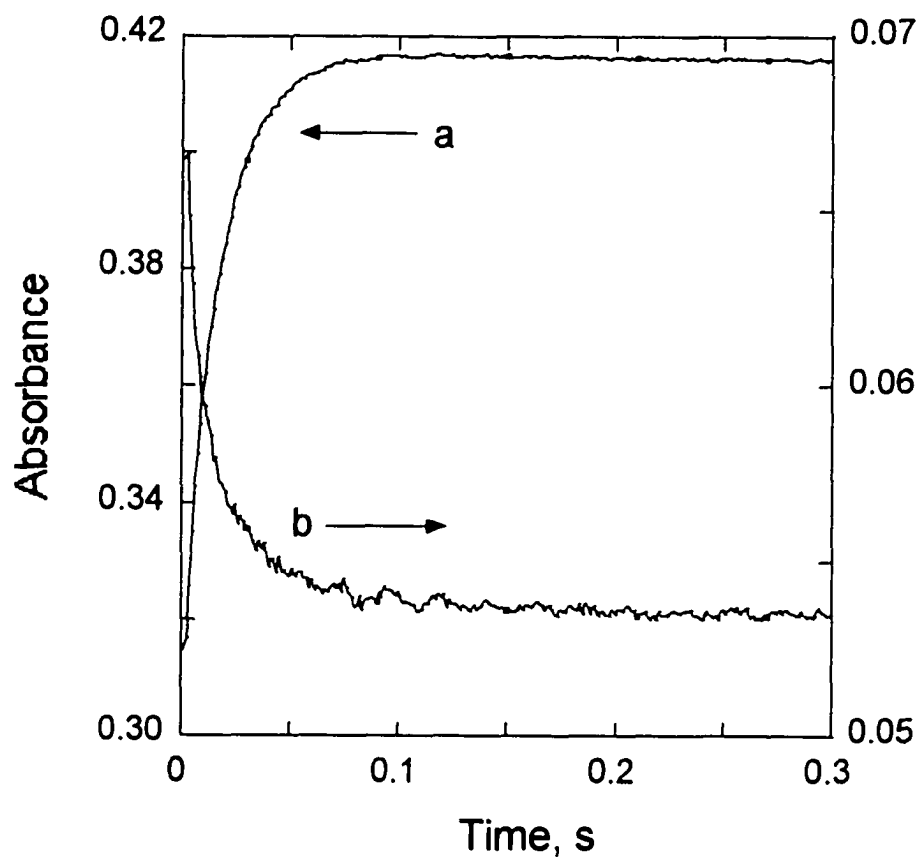


Figure 1. Reaction between 10^{-5} M AcrH₂ and 10^{-4} M Ce⁴⁺. (a) Formation of AcrH⁺ monitored at 358 nm. (b) Decay of AcrH₂⁺ monitored at 640 nm. [H⁺] = 0.10 M, ionic strength = 1.0 M.

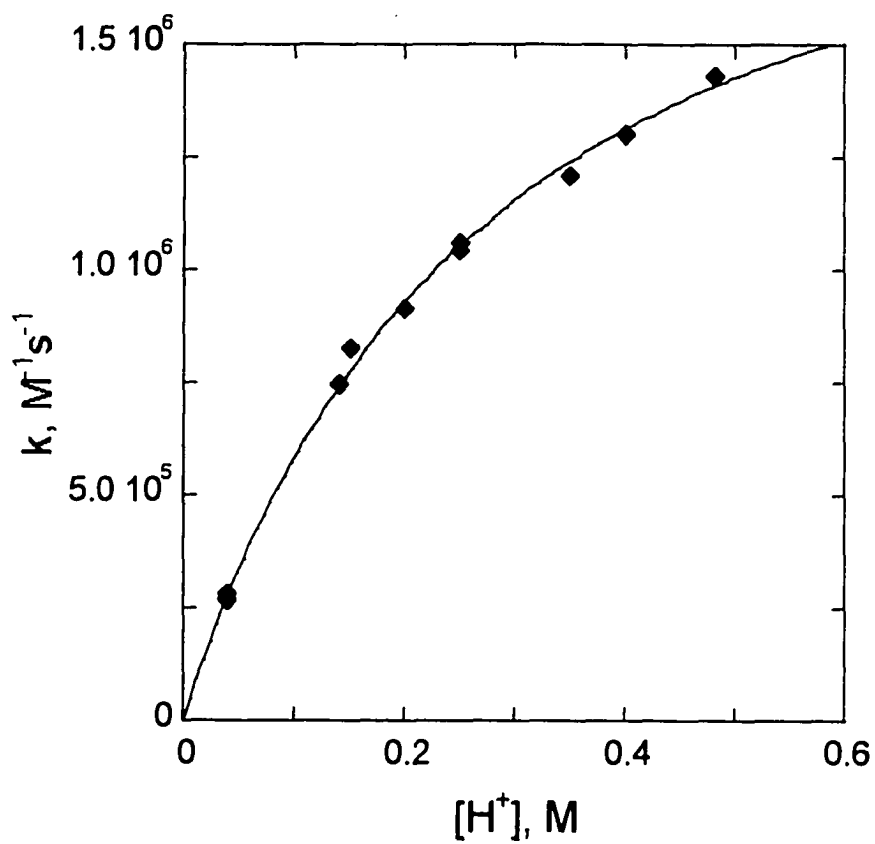
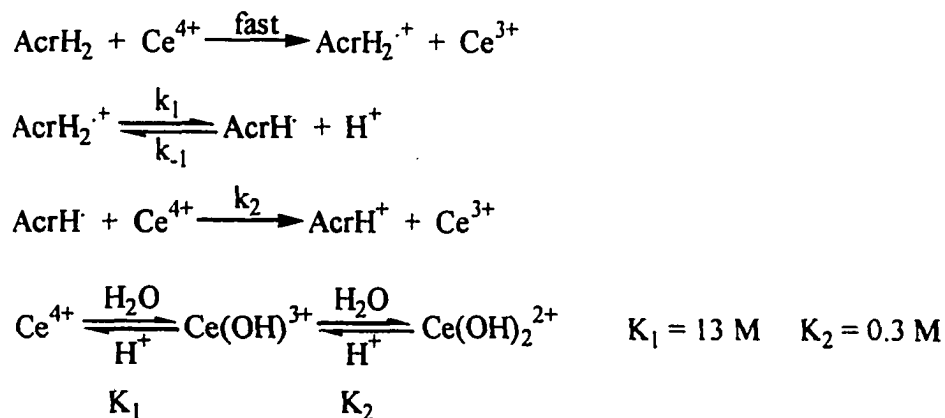


Figure 2. Plot of the second order rate constant against $[\text{H}^+]$ for the reaction between $1.5 \times 10^{-5} \text{ M}$ AcrH_2 and $2 \times 10^{-4} \text{ M}$ Ce^{4+} . Ionic strength = 1.0 M.

Scheme I



The application of the steady state approximation to the concentration of AcrH• yields the following rate law:

$$v = \frac{k_1 k_2 [\text{AcrH}_2^{\cdot+}] [\text{Ce}^{\text{IV}}]_{\text{T}}}{k_{-1} ([\text{H}^+] + K_1 + K_1 K_2 / [\text{H}^+]) + k_2 [\text{Ce}^{\text{IV}}]_{\text{T}}} \quad (3)$$

$$k_{\text{obs}} = \frac{k_1 k_2 [\text{Ce}^{\text{IV}}]_{\text{T}}}{k_{-1} ([\text{H}^+] + K_1 + K_1 K_2 / [\text{H}^+]) + k_2 [\text{Ce}^{\text{IV}}]_{\text{T}}} \quad (3a)$$

Here $[\text{Ce}^{\text{IV}}]_{\text{T}}$ is the total concentration of the ceric ion, and K_1 and K_2 are the first and second acid ionization constants of cerium(IV) ions.¹³

Assuming that the $k_2[\text{Ce}^{\text{IV}}]_{\text{T}}$ term in the denominator is negligible at low ceric ion concentrations, eq 3 reduces to eq 4:

$$v = \frac{k_1 k_2 [\text{AcrH}_2^{\cdot+}] [\text{Ce}^{\text{IV}}]_{\text{T}}}{k_{-1} ([\text{H}^+] + K_1 + K_1 K_2 / [\text{H}^+])} \quad (4) \quad k_{\text{obs}} = \frac{k_1 k_2 [\text{Ce}^{\text{IV}}]_{\text{T}}}{k_{-1} ([\text{H}^+] + K_1 + K_1 K_2 / [\text{H}^+])} \quad (4a)$$

The non-linear least-squares fit of the acid variation data to eq 4a yielded $k_1 k_2 / k_{-1} = (3.04 \pm 0.02) \times 10^7 \text{ s}^{-1}$. Assigning $7.4 \times 10^9 \text{ L mol}^{-1} \text{ s}^{-1}$ as a value of k_2 (see Discussion) gives $\text{p}K_{\text{a}}(\text{AcrH}_2^{\cdot+}) = -\log(k_1 / k_{-1}) = 2.39$.

Saturation kinetics were observed at higher concentrations of Ce^{IV} . **Figure 3** shows a reciprocal plot of the observed pseudo-first order rate constant of the $\text{Ce}^{\text{IV}}/\text{AcrH}_2$ reaction vs. the total ceric ion concentration. The $[\text{Ce}^{\text{IV}}]$ variation data were fitted to eq 5, which was derived by taking a reciprocal of eq 3a and separating the $1/[\text{Ce}^{\text{IV}}]_{\text{T}}$ term:

$$\frac{1}{k_{\text{obs}}} = \frac{1}{k_1} + \frac{k_{-1}([\text{H}^+] + K_1 + K_1K_2/[\text{H}^+])}{k_1 k_2} \frac{1}{[\text{Ce}^{\text{IV}}]_{\text{T}}} \quad (5)$$

This treatment gave $k_1 = 721 \pm 29 \text{ s}^{-1}$ and $k_{-1} = (1.33 \pm 0.03) \times 10^5 \text{ L mol}^{-1} \text{ s}^{-1}$.

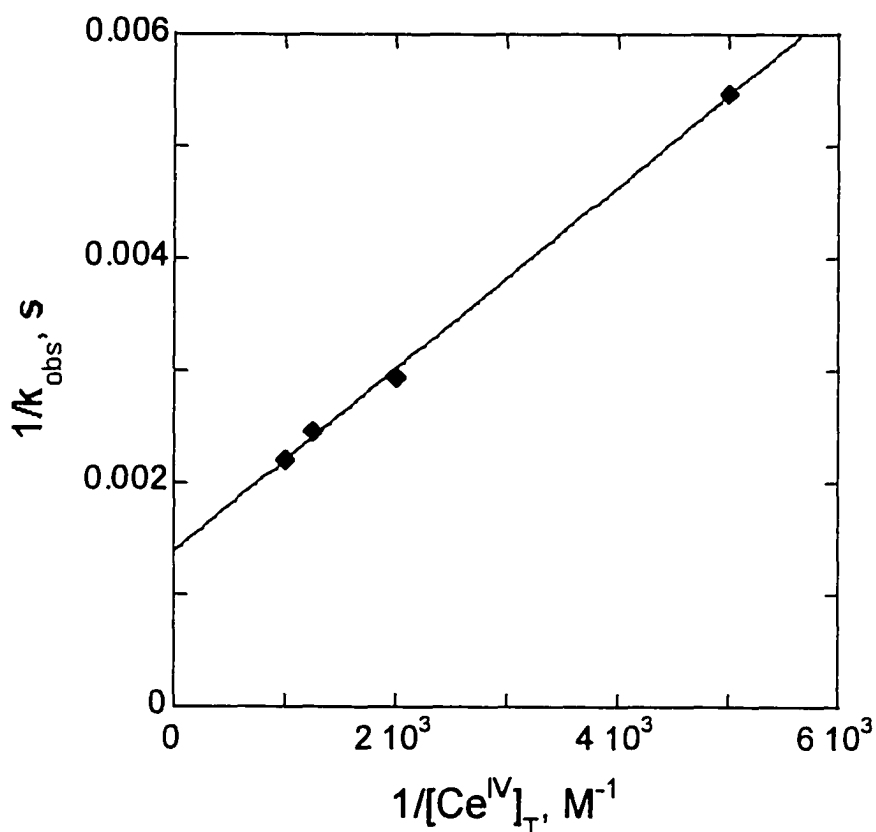


Figure 3. Plot of $1/k_{\text{obs}}$ against $1/[\text{Ce}]_{\text{T}}$ for the reaction between $1.5 \times 10^{-5} \text{ M}$ AcrH_2 and Ce^{4+} . $[\text{H}^+] = 0.2 \text{ M}$, ionic strength = 1.0 M. Figure 3

A global fit of both acid variation and ceric ion variation data was performed. Equation 6 was derived by dividing the numerator and denominator of the right side of eq 3a by $k_2[\text{Ce}^{\text{IV}}]_{\text{T}}$:

$$k_{\text{obs}} = \frac{k_1}{\frac{k_1 ([\text{H}^+] + K_1 + K_1 K_2 / [\text{H}^+])}{k_2 [\text{Ce}^{\text{IV}}]_{\text{T}}} + 1} \quad (6)$$

Figure 4 shows a plot of k_{obs} vs. $([\text{H}^+] + K_1 + K_1 K_2 / [\text{H}^+]) / [\text{Ce}^{\text{IV}}]_{\text{T}}$. The fitting of the data in Figure 4 to eq 6 gave $k_1 = 691 \pm 36 \text{ s}^{-1}$ and $k_{-1} = (1.18 \pm 0.11) \times 10^5 \text{ L mol}^{-1} \text{ s}^{-1}$. A more accurate value of $\text{p}K_{\text{a}}$ for AcrH_2^{2+} was then calculated as $\text{p}K_{\text{a}}(\text{AcrH}_2^{2+}) = -\log(k_1/k_{-1}) = 2.23 \pm 0.05$.

Kinetic isotope effects in Ce(IV) reactions. Reactions of Ce(IV) with $\text{AcrD}_2/\text{AcrH}_2$ were carried out in H_2O or D_2O mixtures with acetonitrile using the $[\text{Ce}^{\text{IV}}]$ variation method. The rate constants k_1 and k_{-1} were calculated from a non-linear least-squares fit of k_{obs} to eq 6. Table 1 summarizes the k_1 and k_{-1} values for $\text{AcrH}_2/\text{AcrD}_2$ reactions with Ce(IV) in H_2O and D_2O .

Table 1. k_1 and k_{-1} rate constants for the reactions between Ce^{IV} and AcrL_2 in $\text{L}_2\text{O}/\text{AN}^{\text{a}}$

Entry	k_1, s^{-1}	$k_{-1} \times 10^{-4}, \text{L mol}^{-1} \text{s}^{-1}$
1 AcrH ₂ in H ₂ O	691 ± 36	11.8 ± 1.1
2 AcrH ₂ in D ₂ O	688 ± 22	9.77 ± 0.67
3 AcrD ₂ in H ₂ O	115 ± 3	2.23 ± 0.25
4 AcrD ₂ in D ₂ O	106 ± 6	3.41 ± 0.58

^a L = H or D

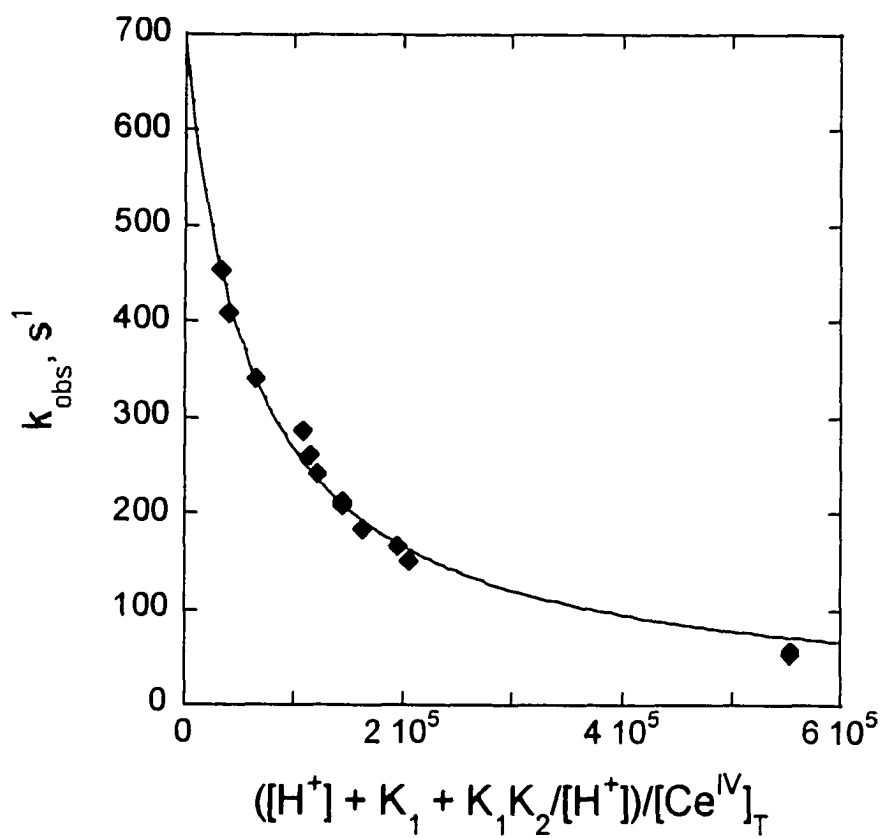


Figure 4. Global fit of acid and ceric ion variation data for the reaction between Ce^{4+} and AcrH_2 . The experimental values of k_{obs} were fitted to equation 6.

A series of experiments with AcrD_2 (10^{-4} M) in D_2O were also carried out at a higher concentration of Ce^{IV} (4×10^{-3} M) and a constant acid concentration (0.4 M). The reaction was monitored in the spectral range from 560 to 720 nm. The resulting absorbance changes and pseudo-first order rate constants obtained from the exponential fitting of the kinetic traces were plotted against the wavelength, **Figure 5**.

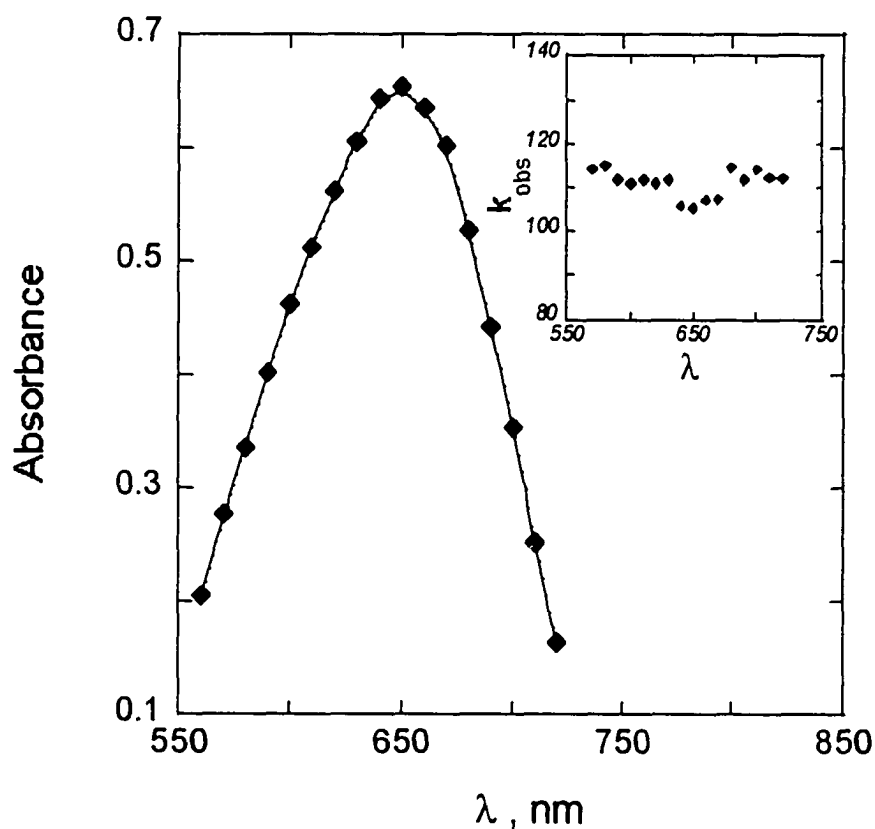


Figure 5. Absorbance changes in the reaction between 10^{-4} M AcrD_2 and 4×10^{-3} M Ce^{4+} . $[\text{H}^+] = 0.4$ M, ionic strength = 1.0 M. Shown as an inset is the plot of the corresponding pseudo-first order rate constants against the wavelength.

Thus obtained spectrum of the acridinium radical cation exhibits a maximum at 650 nm with the extinction coefficient of $6530 \text{ L mol}^{-1} \text{ cm}^{-1}$. The pseudo-first order rate constants vary slightly with the wavelength and approach 106 s^{-1} at the maximum absorbance change, in excellent agreement with the value obtained by the $[\text{Ce}^{\text{IV}}]$ variation method.

Reaction with hexachloroiridate(IV). The stoichiometry of hexachloroiridate(IV) reaction with AcrD_2 was determined spectrophotometrically under air-free conditions. A small excess of iridium complex was allowed to react with AcrD_2 and the spectra of the reaction mixture were recorded before and after the reaction. The excess of IrCl_6^{2-} was calculated from the total absorbance reading at 487 nm. The spectrum of the product was obtained by subtracting the spectrum of the excess of IrCl_6^{2-} from the final spectrum. The resulting spectrum matched that of an authentic sample of AcrD^+ . The overall stoichiometry of the $\text{IrCl}_6^{2-}/\text{AcrD}_2$ reaction was 1.95:1 under air free conditions and $\sim 1.5:1$ in air saturated solutions. Under the latter conditions, the stoichiometry showed a minor dependence on the concentration of the iridium complex. The kinetics of hexachloroiridate(IV) reaction with AcrD_2 were studied in AN/ H_2O mixture using the stopped-flow technique under air free conditions. Typical concentrations used were $(0.50\text{-}1.0) \times 10^{-3} \text{ M IrCl}_6^{2-}$, $5 \times 10^{-5} \text{ M AcrD}_2$ and 0.10 M HClO_4 at 1.0 M ionic strength. The reaction was monitored at 358nm (AcrD^+) and 650nm (AcrD_2^{++}). The reaction followed first order kinetics at both wavelengths and yielded $k_\psi = 115 \pm 2 \text{ s}^{-1}$ independent of the concentrations of IrCl_6^{2-} and H^+ .

In a different set of experiments, AcrH_2 was used instead of AcrD_2 . The concentrations of both IrCl_6^{2-} and AcrH_2 were much lower ($5 \mu\text{M}$ and $2 \mu\text{M}$,

respectively) to allow for the competition between reactions -1 and 2 (Scheme I). The acid concentration was varied from 0.2 to 0.5 M at 1.0 M ionic strength. The reaction was monitored at 358 nm (AcrH^+) and followed pseudo-first order kinetics. Although we were unable to obtain reliable quantitative kinetics data under these conditions due to the limitation of our stopped-flow apparatus, a trend of decreasing rate constants, from ca. 500 to 200 s^{-1} , with increasing acid concentration was observed.

Reaction with aqueous iron(III). The reactions of AcrH_2 and AcrD_2 with Fe^{3+} were monitored in AN/ H_2O mixture under air free conditions using conventional UV-VIS and stopped-flow techniques at 300 nm (AcrH_2), 358 nm (AcrH^+) and 640 nm (AcrH_2^{2+}). In a typical kinetic run, Fe^{3+} (1 mM) was used in a large excess over AcrH_2 or AcrD_2 (5×10^{-5} M). In all of the experiments, the ionic strength was maintained at 1.0 or 0.1 M, and $[\text{H}^+]$ was varied from 0.1 to 0.5 M. No absorbance change was noted at 640 nm. At 300 nm and 358 nm the reaction followed first order kinetics and yielded the same pseudo-first order rate constants, indicating a clean substrate-to-product conversion. The pseudo-first order rate constants were proportional to the Fe^{3+} concentration and independent of the acidity.

The second order rate constants for the reactions of Fe^{3+} with AcrH_2 and AcrD_2 reactions were calculated from a linear plot of k_{ψ} vs. $[\text{Fe}^{3+}]$. At 0.1 and 1.0 M ionic strength, the second order rate constants of $\text{Fe}^{3+}/\text{AcrH}_2$ reaction were 37.9 ± 0.03 and $128 \pm 1 \text{ L mol}^{-1} \text{ s}^{-1}$, respectively. AcrH_2 and AcrD_2 yielded the same rate constants at a given ionic strength, indicating no kinetic isotope effect. No rate inhibition was observed when up to 1 mM Fe^{2+} was added.

Cyclic voltammetry of AcrH₂ in AN and AN/H₂O mixed solvents. Slow-scan cyclic voltammetry was performed on AcrH₂ solutions in pure acetonitrile and 20% AN / 80% H₂O solvent mixture under an argon atmosphere. In both solvents the cyclic voltammograms exhibited anodic waves with current maxima at 0.81 V and 0.46 V (vs. SCE in AN and AN/H₂O, respectively), but the complementary cathodic waves were not observed at scan rates of up to 3 V s⁻¹, **Figure 6**.

Discussion

The reaction of dihydroacridine with Ce(IV) in 20% AN/80% H₂O proceeds in two one-electron transfer steps, **Scheme I**. The first step is fast (not observable on a stopped-flow time scale) and produces a transient radical cation. The further oxidation of the radical cation was observed by monitoring either the product, AcrH^{•+}, or the radical cation itself. Both species exhibit the same kinetic behavior suggesting that no by-products are formed in this reaction.

Since the reduction potential of AcrH^{•+}/AcrH[•] couple is -0.43 V (vs. SCE in acetonitrile)¹⁰ and the oxidation of dihydroacridine ($E(\text{AcrH}_2^{•+}/\text{AcrH}_2) = +0.46 \text{ V vs. SCE}$) by Ce(IV) is too rapid to be monitored by the stopped-flow technique, it was reasonable to assume that the reaction between AcrH[•] and Ce⁴⁺ is diffusion controlled. Therefore we assign $k_2 = 7.4 \times 10^9 \text{ L mol}^{-1} \text{ s}^{-1}$.¹⁴

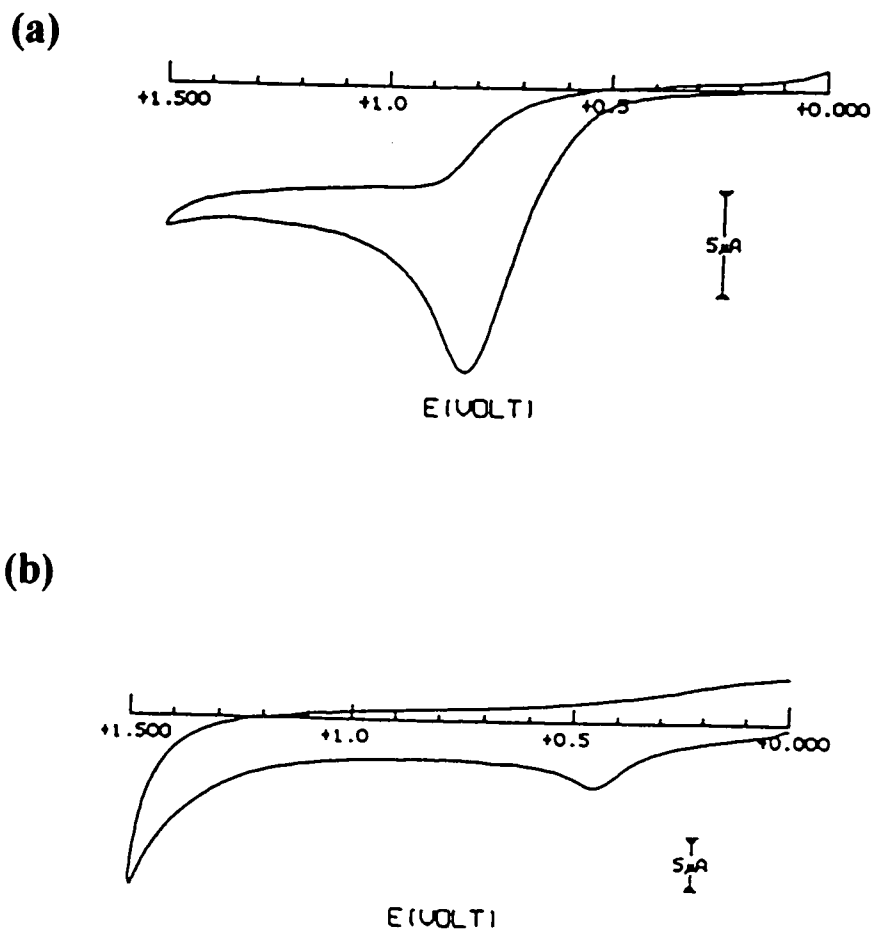
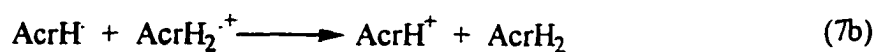


Figure 6. Cyclic voltammograms of AcrH_2 in a) AN, b) 20% AN/80% H_2O at 25 °C.

The fact that Ce(IV) exists mostly in the form of monohydroxy and dihydroxy species at $[H^+] = 0.1 - 0.5 \text{ M}$ ^{13b} has allowed us to study the competition between steps 2 and -1 of **Scheme I** and thus determine the rate constants for the protonation and deprotonation equilibrium of the radical cation. A simple comparison of absolute rates for steps -1 and 2 under conditions where the competition was observed ($[H^+] = 0.3 \text{ M}$, $[Ce]_T = 2 \times 10^{-4} \text{ M}$, $[Ce^{4+}] \sim 2.3 \times 10^{-6} \text{ M}$, $[Ce(OH)^{3+}] \sim 10^{-4} \text{ M}$, $[Ce(OH_2)^{2+}] \sim 10^{-4} \text{ M}$) suggests that the reactive form of ceric ion is Ce^{4+} . This was also confirmed by the acid variation experiments in which the observed dependence of the reaction rates on the acid concentration matched the rate law derived from **Scheme I**.

Although the reaction mechanism depicted in **Scheme I** is very similar to that proposed earlier⁸ in acetonitrile, we did not observe the disproportionation of the radical cation, eq 7a. In fact, it is more reasonable to assume that the second order decay of the radical cation comes from the reaction of $AcrH^\bullet$ with $AcrH_2^{+\bullet}$, eq 7b, a simple one-electron transfer reaction. KinSim simulations have shown that reaction 7b is unimportant under our experimental conditions and cannot contribute significantly to the decay of the radical cation.



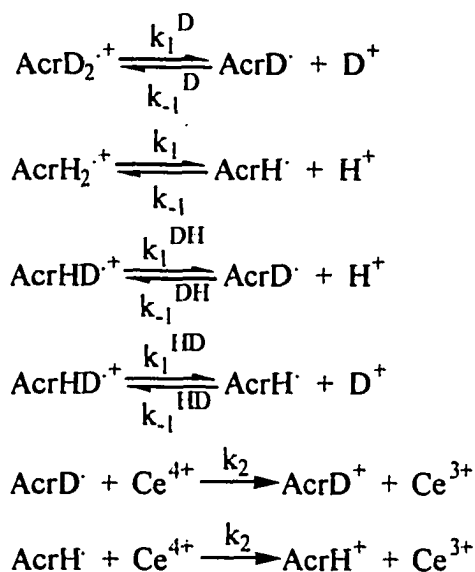
The acid ionization constant $pK_a = 2.23$ for $AcrH_2^{+\bullet}$ is much lower than the values determined earlier at low concentrations of water in acetonitrile ($pK_a = 8.1$ at $[H_2O] = 0.029 \text{ M}$ and 6.8 at $[H_2O] = 0.29 \text{ M}$).^{8,10,15} A linear plot of pK_a vs. $\log [H_2O]$ presented

in ref. 8 allows us to estimate the corresponding pK_a value under our experimental conditions. Considering the degree of approximation used in such an analysis, the calculated value of 3.96 is in acceptable agreement with $pK_a = 2.23$ in 20% AN / 80% H_2O solvent mixture determined directly in this work. It has been noted^{8,16} that water in acetonitrile has a large retardation effect on k_1 and a small acceleration effect on k_{-1} ($k_1 = 6.4 \text{ s}^{-1}$ and $k_{-1} = 8.06 \times 10^8 \text{ L mol}^{-1} \text{ s}^{-1}$ at $[H_2O] = 0.029 \text{ M}$; $k_1 = 11.5 \text{ s}^{-1}$ and $k_{-1} = 7.26 \times 10^7 \text{ L mol}^{-1} \text{ s}^{-1}$ at $[H_2O] = 0.29 \text{ M}$). Our data suggest that both k_1 and k_{-1} change significantly at higher concentrations of H_2O .

Kinetic isotope effects for k_1 and k_{-1} deserve special attention. A kinetic isotope effect of 9.0 for k_1 in acetonitrile has been reported.⁸ From the experiments with $AcrD_2$ and $AcrH_2$ in D_2O and H_2O solvent mixtures with acetonitrile, we have been able to determine the kinetic isotope effects for both k_1 and k_{-1} . From entries 1 and 4 in **Table 1** we calculate $(k_H/k_D)_1 = 6.52 \pm 0.51$ and $(k_H/k_D)_{-1} = 3.45 \pm 0.68$. An apparently low value of k_{-1} in entry 3 of **Table 1** is probably a result of a complex reaction mechanism operating in $AcrD_2/Ce(IV)/H_2O/AN$ system, as explained below.

Conditions in entry 3 of **Table 1** allow isotope scrambling in $AcrD_2^{**}$, **Scheme II**. KinSim simulations have shown that kinetic traces for formation of $AcrL^-$ retain the exponential form under such conditions, but the apparent k_1 depends on the values of k_1^{DH} , k_{-1}^{DH} and k_1^{HD} .

Scheme II



Neglecting any secondary isotope effect on k_1 (see later) and taking the statistically corrected values of $k_1^{\text{DH}} = k_1/2 = 345 \text{ s}^{-1}$ and $k_1^{\text{HD}} = k_1^{\text{D}}/2 = 53 \text{ s}^{-1}$, the data in entry 3 yield $k_{-1}^{\text{DH}} = (6.34 \pm 0.04) \times 10^4 \text{ L mol}^{-1} \text{ s}^{-1}$, **Figure 7**. In these calculations, the value of k_{-1}^{HD} was fixed at $5 \times 10^4 \text{ L mol}^{-1} \text{ s}^{-1}$, but changing it in either direction by a factor of 10 did not affect the fitting due to a relatively small importance of this step. The value of k_{-1}^{DH} was then used to estimate the secondary and solvent isotope effects for k_{-1} separately. We define the secondary kinetic isotope effect for k_{-1} as $(k_{\text{H}}/k_{\text{D}})_{-1}^{\text{sec}} = k_{-1}/k_{-1}^{\text{DH}} = 1.86 \pm 0.17$ and the solvent kinetic isotope effect for k_{-1} as $(k_{\text{H}}/k_{\text{D}})_{-1}^{\text{sol}} = k_{-1}^{\text{DH}}/k_{-1}^{\text{D}} = 1.86 \pm 0.32$. Solvent isotope effects for a system $\text{S} + \text{L}_3\text{O}^+ = \text{SL}^+ + \text{L}_2\text{O}$ have been reported in the literature and usually range from 2.3 to 2.7.¹⁷ The solvent isotope effect for k_1 determined in this study, 1.86 ± 0.32 , is acceptably close, considering the uncertainty in the value. An attempt to fit the experimental data in entry 2 to the mechanism depicted in **Scheme II** was also made. Due to the short timescale of this reaction

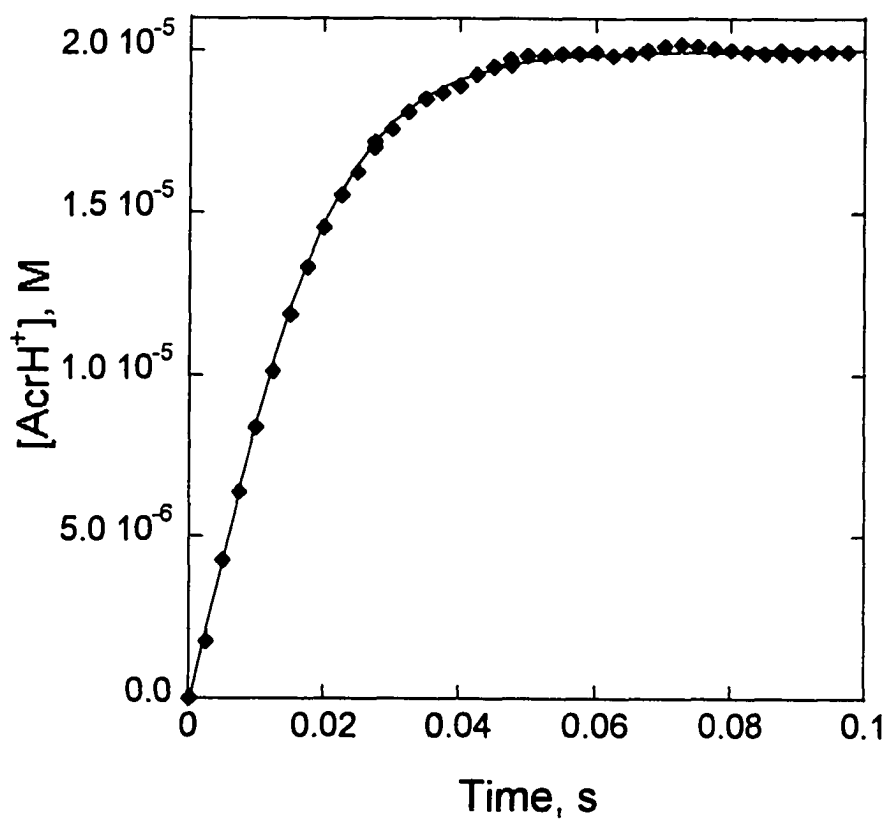


Figure 7. FitSim fit of the reaction between 2×10^{-5} M AcrD₂ with 1.25×10^{-4} M Ce(IV) in H₂O, [H⁺] = 0.3 M. An experimental kinetic trace was fitted to the reaction mechanism in Scheme II.

(ca. 50% completion during the mixing time of our stopped-flow apparatus) we were unable to obtain a satisfactory fit.

A series of FitSim simulations were performed to study the effect of the secondary isotope effect for k_1 on $(k_H/k_D)_{-1}^{sec}$. Arbitrary values of $(k_H/k_D)_{-1}^{sec}$ were used to calculate k_1^{HD} and k_1^{DH} , and the corresponding values of $(k_H/k_D)_{-1}^{sec}$ were obtained from the fitting procedure described above. A trend of increasing $(k_H/k_D)_{-1}^{sec}$ with increasing $(k_H/k_D)_{-1}^{sec}$ was observed, **Table 2**.

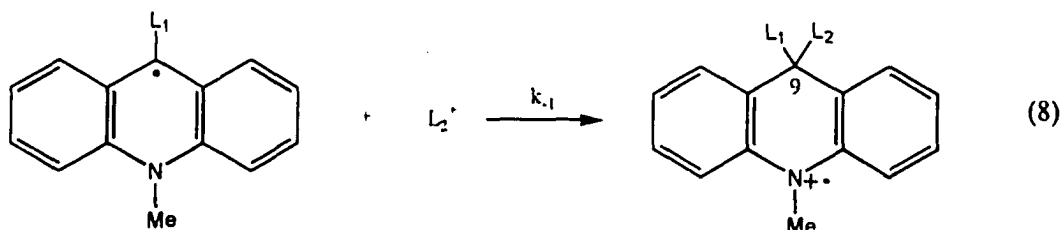
Table 2. Effect of the secondary kinetic isotope effect for k_1 on $(k_H/k_D)_{-1}^{sec}$

$(k_H/k_D)_{-1}^{sec}$	k_1^{HD} , ^a s ⁻¹	k_1^{DH} , ^a s ⁻¹	$(k_H/k_D)_{-1}^{sec}$ ^b
1.0	53.0	345	1.86±0.17
1.1	58.3	314	1.93±0.18
1.2	63.6	288	1.99±0.19

^a Calculated from k_1 and k_1^D based on $(k_H/k_D)_{-1}^{sec}$. ^b Obtained from FitSim fitting

The quality of the fit was visibly worse at higher values (1.1 and 1.2) of $(k_H/k_D)_{-1}^{sec}$. This result suggests that the secondary isotope effect for k_1 is either small or non-existent. This is somewhat surprising, since sizable α -D secondary isotope effects have been seen in similar reactions. A secondary isotope effect of 1.145 ± 0.009 was reported for a hydride abstraction from NADH by 4-cyano-2,6-dinitrobenzenesulfonate.¹⁸ Unusually high α -D isotope effects of 1.38 and 1.50 (no error limits given) have been found for the reductions of acetone and cyclohexanone by various alcohol dehydrogenases.¹⁹

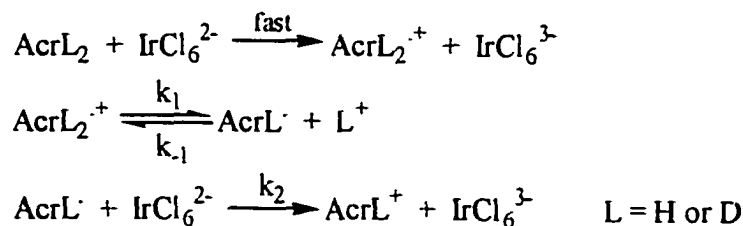
The secondary kinetic isotope effect is due to the presence of the non-transferred L_1 in position 9 of dihydroacridine molecule, eq 8.



Conventional transition state theory predicts a small inverse isotope effect for a conversion of an sp^2 hybridized C-L bond to an sp^3 -like transition state in this reaction.^{17a,20} A hydride transfer to the acridinium cation produces a small normal isotope effect whose magnitude depends on whether H^- or D^- is transferred.^{2c,21} Nuclear tunneling along the reaction coordinate has been proposed to explain such an unusual kinetic behavior of the acridinium ion and some NADH systems.^{21,22} The normal secondary isotope effect observed in this work suggests a possibility of tunneling in the protonation of $AcrH^\bullet$.

Reaction of dihydroacridine with $IrCl_6^{2-}$ proceeds by a mechanism similar to that for $Ce(IV)$, **Scheme III**.

Scheme III

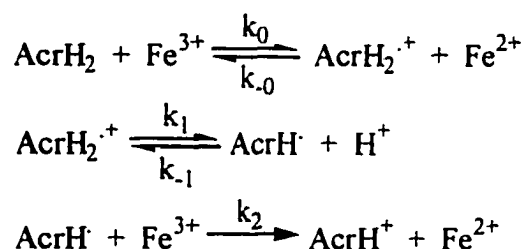


An outer-sphere oxidation of $AcrL_2$ is proposed, based on the products and stoichiometry. Since hexachloroiridate does not form hydroxy species on the time scale of our stopped-

flow experiments¹¹, we were able to obtain the limiting value of k_1 even at the concentrations of IrCl_6^{2-} below 1 mM. The experimental value for k_1 , $115 \pm 2 \text{ s}^{-1}$, is in good agreement with the value of 106 s^{-1} obtained from the $\text{AcrD}_2/\text{Ce(IV)}$ experiments. An attempt at using AcrH_2 with micromolar concentrations of IrCl_6^{2-} to allow for the competition between steps -1 and 2 in Scheme III was not completely successful, but a qualitative trend of increasing rates at lower acid concentrations was observed.

Reaction with Iron(III). Scheme IV shows a proposed mechanism of the reaction between Fe^{3+} and AcrH_2 .

Scheme IV



By using the steady state approximation, one derives the rate law in eq 9.

$$v = \frac{k_0 k_2 [\text{AcrH}_2] [\text{Fe}^{3+}]^2}{k_2 [\text{Fe}^{3+}] + \frac{k_{-0} [\text{Fe}^{2+}]}{k_1} (k_{-1} [\text{H}^+] + k_2 [\text{Fe}^{3+}])} \quad (9)$$

As shown below, this rate law reduces to eq 10 under our experimental conditions and the experimental second order rate constants are in fact k_0 .

$$v = k_0 [\text{AcrH}_2] [\text{Fe}^{3+}] \quad (10)$$

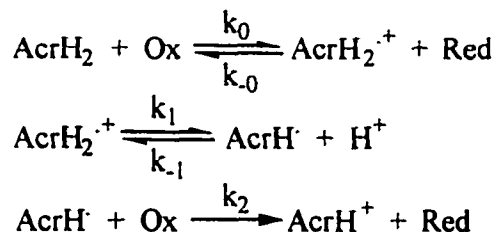
At $[\text{H}^+] = 0.1 - 0.5 \text{ M}$ and $[\text{Fe}^{3+}] = (5 - 20) \times 10^{-4} \text{ M}$, assuming that $k_2 [\text{Fe}^{3+}] \gg k_{-1} [\text{H}^+]$ (this requires $k_2 \gg 10^8 \text{ L mol}^{-1} \text{ s}^{-1}$), we can neglect the $k_{-1} [\text{H}^+]$ term in the denominator of eq 9. k_0 can be calculated from the equilibrium constant $K = k_0/k_{-0} = 15$ (estimated from

the reduction potentials for $\text{Fe}^{3+}/\text{Fe}^{2+}$ and $\text{AcrH}_2^{•+}/\text{AcrH}_2$ couples).²³ From the value of K and the experimental value of k_0 at 1 M ionic strength we obtain $k_{-0} = k_0/K \approx 9 \text{ L mol}^{-1} \text{ s}^{-1}$. Even under the most unfavorable conditions in reaction of AcrD_2 with Fe^{3+} (5×10^{-4} M) with 1 mM of added Fe^{2+} , the term $k_{-0}[\text{Fe}^{2+}]/k_1 = 9 \times 10^{-3} / 106 = 8.5 \times 10^{-5} \ll 1$. The denominator of eq 9 reduces to $k_2 [\text{Fe}^{3+}]$, resulting in the simplified rate law in eq 10. The absence of acid dependence and of the kinetic isotope effect on the rates of $\text{AcrH}_2/\text{Fe}^{3+}$ reaction also confirm the validity of **Scheme IV**.

General mechanism of one-electron oxidation of dihydroacridine. Scheme V

represents a unified mechanism for the electron transfer oxidation of dihydroacridine.

Scheme V



The first step in **Scheme V** is a reversible one-electron oxidation of dihydroacridine to the radical cation $\text{AcrH}_2^{•+}$. The consecutive loss of H^+ and further oxidation of AcrH^{\bullet} complete the mechanism. Depending on the reduction potential of the oxidant, either of the first two reaction steps can be rate-determining. Strong oxidizing reagents with high self-exchange rate constants, such as Ce(IV) or IrCl_6^{2-} ,^{24,25} make step 0 practically irreversible and too rapid to be observed by the stopped-flow technique. Consequently, one can study the kinetics and chemical behavior of $\text{AcrH}_2^{•+}$ as step 1 becomes rate-limiting. In the reaction with Fe^{3+} , which is a mild oxidant and has a small self-exchange rate constant²⁶, step 0 becomes rate-limiting. Another example of such kinetic behavior

was observed in the reaction between AcrH₂ and chromate under similar conditions ([H⁺] = 0.1 M, 20% AN/80% H₂O mixed solvent).²⁷ Both hydrogen chromate and dichromate react with AcrH₂ in a complex chain reaction with the initiation step being one-electron oxidation of AcrH₂, eq 11.



Given the low standard reduction potential of Cr^{VI}/Cr^V couple²⁸, it is not surprising that the initial electron transfer from AcrH₂ to chromate is rate-limiting.

Acknowledgement

This work was supported by a grant from the National Science Foundation (CHE-9007283). Some experiments were conducted with the use of the facilities of the Ames Laboratory. We wish to thank Dr. Victor Adamian for the help with the cyclic voltammetry experiments.

References

- (12) (a) Eisner, U.; Kuthan, J. *Chem. Rev.* **1972**, *72*, 1. (b) Stout, D. M.; Mayer, A. I. *Ibid.* **1982**, *82*, 223. (c) Shinkai, S.; Bruice, T. *Biochemistry* **1973**, *12*, 1750. (d) Kurz, L.; Frieden, C. *J. Am. Chem. Soc.* **1975**, *97*, 667. (e) Jones, J.; Taylor, K. *Can. J. Chem.* **1976**, *54*, 2974.
- (13) (a) Ohnishi, Y.; Ohno, A. *Chem. Lett.* **1976**, 697. (b) Kill, R.; Widdowson, D. *J. Chem. Soc., Chem. Commun.* **1976**, 697. (c) van Eikeren, P.; Grier, D. *J. Am. Chem.*

- Soc.* 1977, 99, 8057. (d) Hajdu, J.; Sigman, D. *Ibid.* 1976, 98, 6060. (e) Schmamel, C.; Santhanathan, K.; Elving, P. *J. Electrochem. Soc.* 1974, 121, 345.
- (14) (a) Kosower, E. M. In *Free Radicals in Biology*; Pryor, W. A., Ed.; Academic Press: New York, 1976; Vol. II, p 1. (b) Kill, R. J.; Widdowson, D. A. In *Bioorganic Chemistry*; van Tamelen, E. E., Ed.; Academic Press: New York, 1978; Vol. IV, p 239. (c) Bruice, T. C. In *Progress in Bioinorganic Chemistry*; Kaiser, F. T., Kezdy, F. J., Eds.; Wiley: New York, 1976; Vol. IV, p 1. (d) Yasui, S.; Ohno, A. *Bioorg. Chem.* 1986, 14, 70.
- (15) (a) Roberts, R. M. G.; Ostovic, D.; Kreevoy, M. M. *J. Org. Chem.* 1983, 48, 2053. (b) Blaedel, W. J.; Haas, R. G. *Anal. Chem.* 1970, 42, 918. (c) Sinha, A.; Bruice, T. C. *J. Am. Chem. Soc.* 1984, 106, 7291. (d) Fukuzumi, S.; Hironaka, K.; Tanaka, T. *Ibid.* 1983, 105, 4722.
- (16) (a) Fukuzumi, S. In *Advances in Electron Transfer Chemistry*; Mariano, P. S., Ed.; JAI Press: Greenwich, 1992; Vol. 2, p 65. (b) van Eikeren, P.; Grier, D. L. *J. Am. Chem. Soc.* 1976, 98, 4655. (c) Fukuzumi, S.; Kuroda, S.; Goto, T.; Ishikawa, K.; Tanaka, T. *J. Chem. Soc., Perkin Trans. II* 1989, 1047. (d) Fukuzumi, S.; Ishikawa, M.; Tanaka, T. *J. Chem. Soc., Perkin Trans.* 1989, 1037. (e) Ishikawa, K.; Fukuzumi, S.; Goto, T.; Tanaka, T. *J. Am. Chem. Soc.* 1990, 112, 1577. (f) Fukuzumi, S.; Chiba, M.; Tanaka, T. *Chem. Lett.* 1989, 31. (g) Fukuzumi, S.; Mochizuki, S.; Tanaka, T. *J. Am. Chem. Soc.* 1989, 111, 1497. (h) Fukuzumi, S.; Mochizuki, S.; Tanaka, T. *Inorg. Chem.* 1990, 29, 653. (i) Fukuzumi, S.; Tokuda, Y. *J. Phys. Chem.* 1993, 97, 3737.

- (17) (a) van Eikeren, P.; Grier, D. L.; Eliason, J. *J. Am. Chem. Soc.* **1979**, *101*, 7406.
(b) Kim, C. S. Y.; Chaykin, S. *Biochemistry* **1968**, *7*, 2339. (c) Fukuzumi, S.; Ishikawa, M.; Tanaka, T. *Tetrahedron* **1986**, *42*, 1021.
- (18) Powell, M. F.; Wu, J. G.; Bruice, T. C. *J. Am. Chem. Soc.* **1984**, *106*, 3850.
- (19) Fukuzumi, S.; Tokuda, Y.; Kitano, T.; Okamoto, T.; Otera, J. *J. Am. Chem. Soc.* **1993**, *115*, 8960.
- (20) Karrer, P.; Szabo, L.; Krishna, H. Y. V.; Schwyzer, R. *Helv. Chim. Acta* **1950**, *XXXIII*, 294.
- (21) Fukuzumi, S.; Koumitsu, S.; Hironaka, K.; Tanaka, T. *J. Am. Chem. Soc.* **1987**, *109*, 305.
- (22) Sykes, A. G.; Thorneley, R. N. F. *J. Chem. Soc. (A)* **1970**, 232.
- (23) Carlyle, D. W.; Espenson, J. H. *Inorg. Chem.* **1967**, *6*, 1370.
- (24) (a) Sherrill, M. S.; King, C. B.; Spooner, R. C. *J. Am. Chem. Soc.* **1943**, *65*, 170.
(b) Boes, C. F., Jr.; Mesmer, R. E. *The Hydrolysis of Cations*; Wiley: New York, 1976. (c) Offner, H. G.; Skoog, D. A. *Anal. Chem.* **1966**, *38*, 1520. (d) Adamson, M. G.; Dainton, F. S.; Glentworth, P. *Trans. Faraday. Soc.* **1965**, *61*, 689. (e) Sillen, L. G.; Martell, A.E., Eds.; *Spec. Publ. - Chem. Soc.* **1964**, No. 17.
- (25) Espenson, J. H. In *Chemical Kinetics and Reaction Mechanisms*; McGraw-Hill: New York, 1995; p 201.
- (26) Hapiot, P.; Moiroux, J.; Savéant, J. -M. *J. Am. Chem. Soc.* **1990**, *112*, 1337.
- (27) Sawyer, D. T.; Valentine, J. S. *Acc. Chem. Res.* **1981**, *14*, 393.
-

- (28) (a) Saunders, W. H., Jr. In *Techniques of Chemistry*, Bernasconi, C. F., Ed.; Wiley: New York, 1986; Vol. VI, p 603. (b) Melander, L.; Saunders, W. H., Jr. In *Reaction Rates of Isotopic Molecules*, Wiley: New York, 1980; p 217.
- (29) Kurz, L.; Frieden, C. *J. Am. Chem. Soc.* **1980**, *102*, 4198.
- (30) (a) Cook, P. F.; Oppenheimer, N. J.; Cleland, W. W. *Biochemistry* **1981**, *20*, 1817. (b) Cook, P. F.; Blanchard, J. S.; Cleland, W. W. *Ibid.* **1980**, *19*, 4853. (c) Cook, P. F.; Cleland, W. W. *Ibid.* **1981**, *20*, 1797. (d) Cook, P. F.; Cleland, W. W. *Ibid.* **1981**, *20*, 1805.
- (31) (a) Lu, D. -H.; Maurice, D.; Truhlar, D. G. *J. Am. Chem. Soc.* **1990**, *112*, 6206. (b) Bilkadi, Z.; de Lorimier, R.; Kirsch, J. F. *Ibid.* **1975**, *97*, 4317. (c) Saunders, W. H., Jr. *Ibid.* **1985**, *107*, 164.
- (32) Ostovic, D.; Roberts, R. M. G.; Kreevoy, M. M. *J. Am. Chem. Soc.* **1983**, *105*, 7629.
- (33) Huskey, W. P.; Schowen, R. L. *J. Am. Chem. Soc.* **1983**, *105*, 5704.
- (34) We assume that the irreversible reduction potential determined in the cyclic voltammetry experiments is close to the standard reduction potential. This assumption seems to be valid for the oxidation of AcrH₂ in pure AN (see Ref. 8).
- (35) Duke, F. R.; Parchen, F. R. *J. Phys. Chem.* **1956**, *78*, 1540.
- (36) Hurwitz, P.; Kustin, K. *Trans. Faraday. Soc.* **1966**, *62*, 427.
- (37) (a) Brunshwig, B. S.; Creutz, C.; Macartney, D. H.; Sham, T. -K.; Sutin, N. *Faraday. Discuss. Chem. Soc.* **1982**, *74*, 113. (b) Jolley, W. H.; Stranks, D. R.; Swaddle, T. W. *Inorg. Chem.* **1990**, *29*, 1948.
- (38) Pestovsky, O.; Bakac, A.; Espenson, J. H., manuscript in preparation.

- (39) Rahman, M.; Rocek, J. *J. Am. Chem. Soc.* **1971**, *93*, 5462.

CHAPTER II

REACTIONS OF 10-METHYL-9,10-DIHYDROACRIDINE WITH

CHROMATE

A paper to be submitted to the *Journal of the American Chemical Society*

Oleg Pestovsky, Andreja Bakac and James H. Espenson

Abstract

The oxidation of AcrH₂ to AcrH⁺ by hydrogen chromate ions is a chain reaction that is strongly inhibited by oxygen. The initiation reaction between AcrH₂ or AcrD₂ and H₂CrO₄ forms AcrH₂^{•+} and occurs by a 1e mechanism, $k^H = k^D = 4.6 \times 10^2 \text{ L mol}^{-1} \text{ s}^{-1}$ (25 °C). The Cr^V produced along with AcrH[•] (from the acid ionization of AcrH₂^{•+}) are chain-carrying intermediates. The propagating reaction between AcrH₂ and Cr^V, $k = 1 \times 10^8 \text{ L mol}^{-1} \text{ s}^{-1}$, is of key importance since it is a branching reaction that yields two chain carriers, AcrH[•] and CrO²⁺, by hydrogen atom abstraction. The same partners react competitively by hydride ion abstraction, to yield Cr³⁺ and AcrH⁺, $k = 1.2 \times 10^7 \text{ L mol}^{-1} \text{ s}^{-1}$, in the principal termination step. The reaction of CrO²⁺ and AcrH₂, $k^H = 1.0 \times 10^4$ and $k^D = 4.8 \times 10^3 \text{ L mol}^{-1} \text{ s}^{-1}$, proceeds by hydride ion transfer. The Cr²⁺ so produced could be trapped as CrOO²⁺ when O₂ was present, thereupon terminating the chain. AcrH₂ itself reacts with Cr₂O₇²⁻ + H⁺, $k = 5.6 \times 10^3 \text{ L}^2 \text{ mol}^{-2} \text{ s}^{-1}$, but this step is not an

initiating reaction. From that, two successive electron transfer steps are believed to occur, yielding $\text{Cr}^{\text{IV}} + \text{Cr}^{\text{VI}} + \text{AcrH}^+$.

Introduction

Dihydronicotinamide adenine dinucleotide (NADH) and its analogs have attracted considerable interest due to their biological importance in electron-transfer reactions, in which these dihydropyridines serve as one- or two-electron reductants in various enzymatic processes.¹ One-electron, hydride and hydrogen atom transfer mechanisms have been proposed for biological and artificial redox reactions of dihydropyridines.² Due to the instability of dihydropyridines towards acid-catalyzed hydrolysis,³ the majority of mechanistic studies have employed 10-methyl-9,10-dihydroacridine (AcrH_2) and its substituted analogs which have been shown to be stable in acidic aqueous and semi-aqueous media.⁴ Recently Fukuzumi et al⁵ have characterized 9-substituted dihydroacridine radical-cations ($\text{AcrH}_2^{\bullet+}$) in acetonitrile (AN) which were believed to be transient intermediates in biological reactions where a one-electron oxidation mechanism applies.⁶ However, no information on the reactivity of such radical-cation intermediates in aqueous media has so far been reported.

Dihydroacridine has proven to be an excellent kinetic probe for monitoring $\text{Cr}(\text{IV})$ and $\text{Cr}(\text{V})$ species which are proposed to be important intermediates in various organic oxidations with chromate.^{7,8} Although aqua chromyl(IV) (CrO_2^{2+}) has been characterized in terms of its properties and reactivity,⁹ the instability of the $\text{Cr}(\text{V})$

intermediates derived from chromate has precluded the direct determination of their properties. The transient complex $\text{trans}-(\text{H}_2\text{O})\text{LCrO}^{3+}$ ($\text{L}=[14]\text{janeN}_4$) undergoes one-electron oxidation reactions with various organic and inorganic reducing reagents.¹⁰ Several other stable Cr(V) complexes employing chelating and macrocyclic ligands to stabilize this unusual oxidation state have been reported.¹¹ Since mechanistic or kinetic data are not available for the redox reactions of Cr(V) intermediates derived from simple chromate, it is desirable to obtain more data concerning the fundamental properties and reactivity of such species.

Here we propose a detailed mechanism for the reaction between 9-methyl-9,10-dihydroacridine and chromate ions in a mixed acetonitrile-water solvent. By applying conventional UV-VIS spectrophotometry and stopped-flow techniques, Cr(IV) and Cr(V) species could be identified as important intermediates in this system. From the implications of the chain-reaction mechanism found to operate in this system in the absence of oxygen, we have been able to determine the reactivities of Cr(IV) and Cr(V) intermediates in competitive electron transfer, hydrogen atom abstraction, and hydride transfer. Also to be noted is a specific inhibiting effect of oxygen which is different from the effect reported by Bruice et al.¹² in the oxidation of dihydropyridines with ferricyanide, which arises from the reaction between pyridinium radicals and O_2 .

Experimental Section

Materials. Perchloric acid, acetonitrile, d_3 -acetonitrile, methanol, zinc metal, potassium dichromate, deuterium oxide, methyl iodide, lithium aluminumhydride, lithium

alumodeuteride, 10-methylacridone and acridine were obtained from commercial sources and used as received. Aqueous solutions of Cr(II) were prepared by reduction of chromium(III) perchlorate with zinc amalgam under anaerobic conditions in aqueous 0.10 M HClO₄. High purity water was obtained by passing laboratory-distilled water through a Millipore-Q purification system. Lithium perchlorate was recrystallized from water three times. 10-Methyl-9,10-dihydroacridine (AcrH₂) and its 9,9'-dideuterated analog AcrD₂ were prepared by reduction of 10-methylacridone with LiAlH₄ or LiAlD₄, respectively, according to the literature procedure.¹³ 10-Methylacridinium iodide was prepared by the reaction of acridine with MeI according to a standard procedure.¹⁴ The purity of the organic starting materials was checked by ¹H-NMR spectroscopy.

Kinetic studies and instrumentation. All the kinetic studies were carried out in a 20% AN-80% H₂O solvent mixture. The ionic strength of the reaction solutions was maintained at 1.0 M by addition of lithium perchlorate. The temperature was controlled at 25.0±0.2 °C. The UV-vis experiments were performed with use of a Shimadzu UV-3101 PC instrument at ambient temperature. The stopped-flow experiments were performed with an Applied Photophysics stopped-flow apparatus under anaerobic conditions. Concentrations of AcrH₂ stock solutions were determined spectrophotometrically, $\epsilon_{285} = 13,200 \text{ L mol}^{-1} \text{ cm}^{-1}$. Stock solutions of potassium dichromate were standardized by weight. Chromyl ion (CrO²⁺) solutions were prepared in situ at pH = 1.0 by stopped-flow mixing of oxygen-free solutions of Cr²⁺ (0.20-0.40 mM) with air-saturated solutions of a substrate used in the experiment.^{9a} The superoxochromium(III) ion (CrO₂²⁺) was identified by its absorption maximum in UV at

290 nm, $\epsilon_{290} = 3000 \text{ L mol}^{-1} \text{ cm}^{-1}$.⁹ Kinetics data were analyzed by least-squares fitting; the KaleidaGraph v3.09 for PC software package was used. NMR and ESR spectroscopic data were obtained by use of a Bruker 400 and Bruker ER 200 D-SRC instruments, respectively. Kinetic simulations were performed with the use of a software package KinSim v.4.0 for PC on a Dell XPSPPro computer.

Results

Stoichiometry of the reaction between AcrH₂ and chromate. Reactions of AcrH₂ with chromate were monitored by conventional UV-vis spectrophotometry. An excess of AcrH₂ (10:1 and 2:1, [AcrH₂] = 2×10^{-4} and 1×10^{-4} M, [Cr^{VI}] = 2×10^{-5} and 5×10^{-5} M) was used to determine the stoichiometry. Under air-free conditions, the reaction occurred during mixing and the amount of AcrH⁺ produced was determined from its absorbance at either 358 or 417 nm. At the two wavelengths, the stoichiometry was AcrH₂:Cr^{VI} = 2.88:2 and 2.94:2, respectively (approximately 3:2).

A series of experiments was performed to investigate the effect of methanol on the yield of AcrH⁺ produced under air-free conditions ([AcrH₂] = 2×10^{-4} M, [Cr^{VI}] = 2×10^{-5} M, [MeOH] = 0.83 and 2.5 M). The yields of AcrH⁺ decreased with increasing concentration of methanol, 68% and 57% at 0.83 and 2.5M MeOH, respectively, compared to the reaction without methanol.

When oxygen-saturated solutions were used under otherwise the same experimental conditions, the reaction was slower and could be monitored by following the buildup of AcrH⁺. With the 10:1 starting AcrH₂:Cr^{VI} ratio, the reaction exhibited biphasic behavior at 417 nm, **Figure 1**. When monitored at 320 nm, the isosbestic point

of AcrH_2 and AcrH^+ , $\epsilon_{320}(\text{AcrH}_2) = \epsilon_{320}(\text{AcrH}^+) = 2,750 \text{ L mol}^{-1} \text{ cm}^{-1}$, the consumption of chromate ($\epsilon_{320} = 770 \text{ L mol}^{-1} \text{ cm}^{-1}$) was shown to be complete in $\sim 500 \text{ s}$, **Figure 2**. The slow linear increase in absorbance at 417 nm at times $> 500 \text{ s}$ can be attributed to the reaction of AcrH_2 with oxygen. This was confirmed in an independent experiment that had no chromate. The kinetic traces at 417 nm were fitted to the rate law of eq 1.

$$(\text{Abs}_t - \text{Abs}_0) = \Delta\text{Abs} [1 - \exp(-k_\psi t)] + m t \quad (1)$$

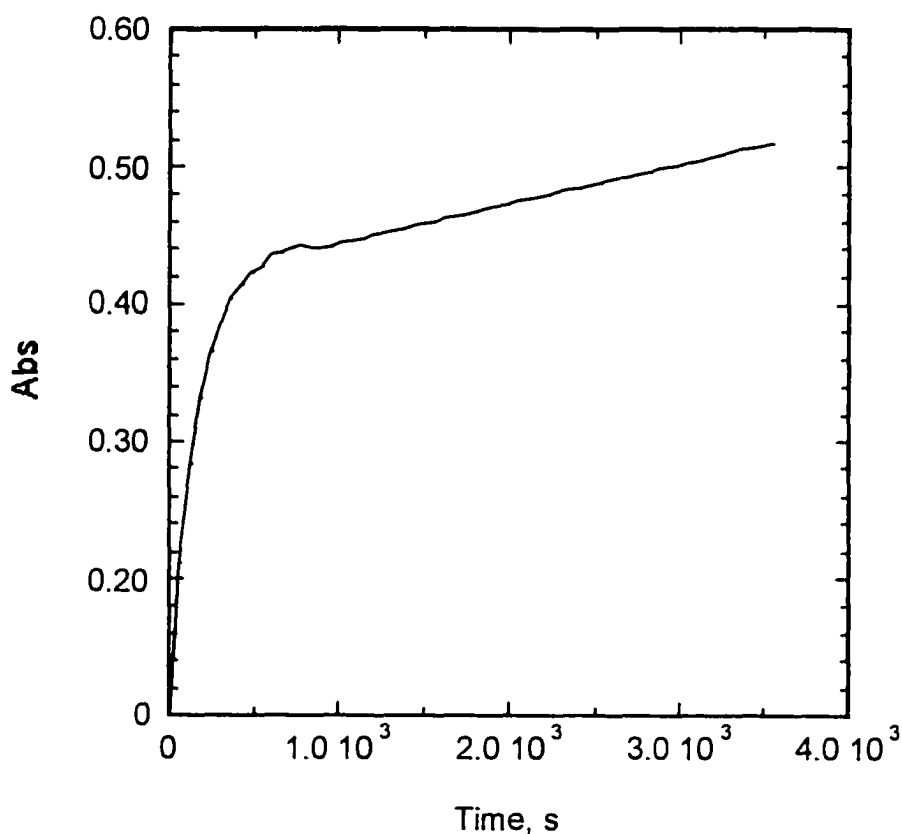


Figure 1. Reaction of AcrH_2 ($2 \times 10^{-4} \text{ M}$) with chromate ($5 \times 10^{-5} \text{ M}$) monitored at 417 nm . $\text{pH} = 1$, $\mu = 1 \text{ M}$, oxygen saturated solution. The slower linear part of the trace is due to the reaction between AcrH_2 and oxygen.

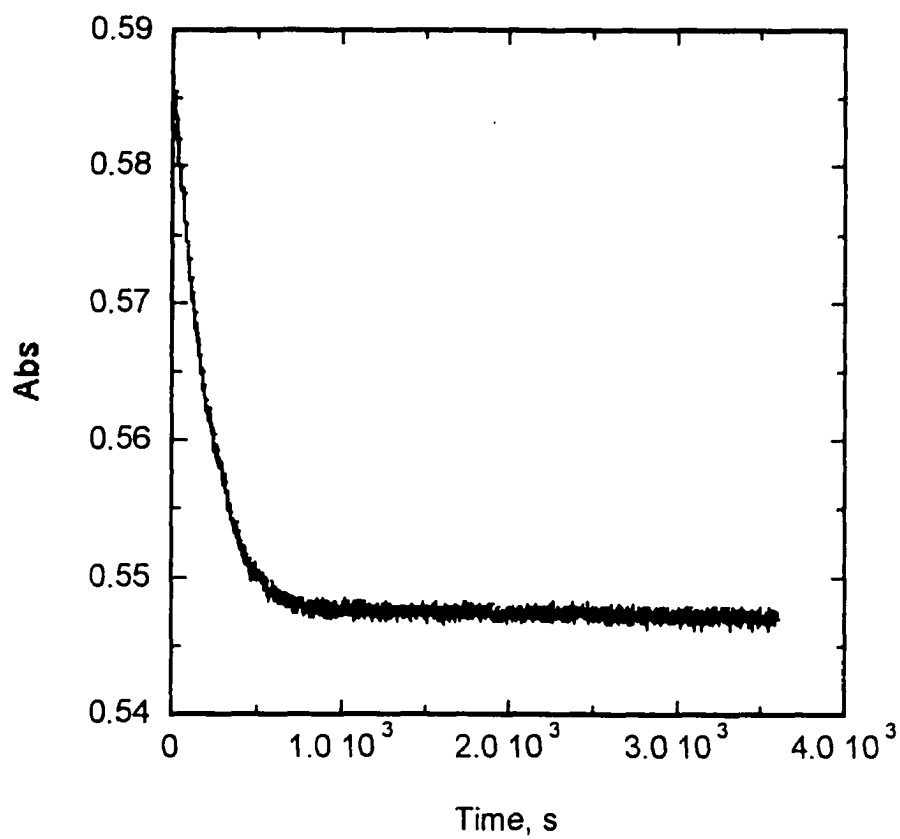


Figure 2. Reaction of AcrH_2 (2×10^{-4} M) and chromate (5×10^{-5} M), $\text{pH} = 1$, $\mu = 1$ M, oxygen saturated solution. Consumption of chromate monitored at 320 nm, the isosbestic point for $\text{AcrH}_2/\text{AcrH}^+$ system.

The amplitude of the exponential term, ΔAbs , was then used to calculate the amount of AcrH^+ produced in the reaction with chromate. The stoichiometry in O_2 saturated solutions was found to be $\text{AcrH}_2:\text{Cr}^{\text{VI}} = 1.88:1$ (approximately 2:1).

Kinetics of the reaction between AcrH_2 and chromate in oxygen- and air-saturated solutions. The data obeyed the pseudo-first-order rate law when a large excess of chromate was used ($[\text{AcrH}_2] = 2 \times 10^{-5} \text{ M}$, $[\text{Cr}^{\text{VI}}] = (2 - 17.5) \times 10^{-4} \text{ M}$). In order to investigate the $[\text{H}^+]$ effect on the rates of the reaction, a series of experiments was performed with varying acid concentration, **Figure 3**. Under all conditions, the reaction rates were proportional to $[\text{H}^+]$. Another series of experiments with varying chromate concentration showed a nonlinear dependence, **Figure 4**. The parabolic behavior of the rate constants with varying chromate concentration was attributed to participation of dichromate in the rate law. The data from **Figure 4** were fitted to the rate law in eq 2.

$$k_{\psi} = 2 [\text{H}^+] (k_{11} [\text{HCrO}_4^-] + k_{12} [\text{Cr}_2\text{O}_7^{2-}]) = [\text{H}^+] (k_{11} [\text{Cr}^{\text{VI}}]_{\text{T}} + K_{\text{d}} k_{12} [\text{Cr}^{\text{VI}}]_{\text{T}}^2) \quad (2)$$

where k_{11} and k_{12} are rate constants of the reactions of AcrH_2 with hydrogen chromate and dichromate, respectively, $K_{\text{d}} = 98 \text{ M}^{-1}$ is the equilibrium constant for dimerization of hydrogen chromate ion ($2 \text{HCrO}_4^- \rightleftharpoons \text{Cr}_2\text{O}_7^{2-} + \text{H}_2\text{O}$),¹⁵ and 2 is the stoichiometric factor. The fitting yielded $k_{11} = (1.12 \pm 0.04) \times 10^2 \text{ L}^2 \text{ mol}^{-2} \text{ s}^{-1}$ and $k_{12} = (5.6 \pm 0.3) \times 10^3 \text{ L}^2 \text{ mol}^{-2} \text{ s}^{-1}$.

When excess of AcrH_2 was used, the reaction followed mixed first-order and linear kinetics, eq 1. **Figure 5** shows a linear plot of the pseudo-first-order rate constants k_ψ obtained from the fitting of the kinetic traces to eq 1 against the acid concentration. A similar plot of k_ψ against $[\text{AcrH}_2]$ was not linear due to interference of the reaction

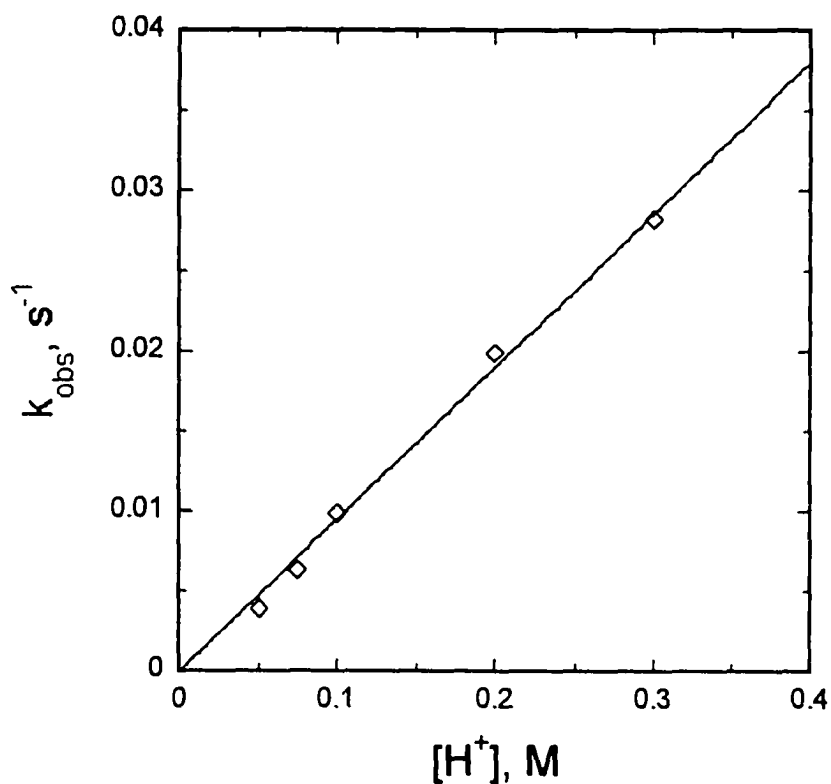


Figure 3. Acid effect in the reaction between AcrH_2 ($2 \times 10^{-5} \text{ M}$) and chromate ($2 \times 10^{-4} \text{ M}$), $[\text{H}^+] = 0.05 - 0.3 \text{ M}$, $\mu = 1 \text{ M}$, oxygen saturated solution.

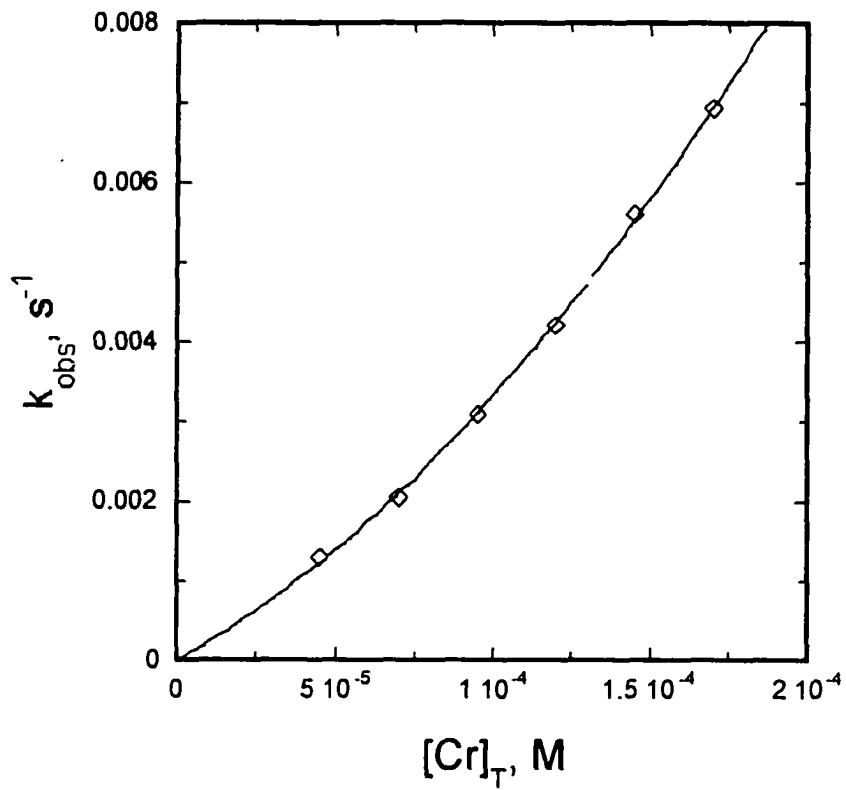


Figure 4. Chromate variation in the reaction between AcrH_2 (2×10^{-5} M) and $(5 - 17.5) \times 10^{-5}$ M chromate, $\text{pH} = 1$, $\mu = 1\text{M}$, oxygen saturate solution.

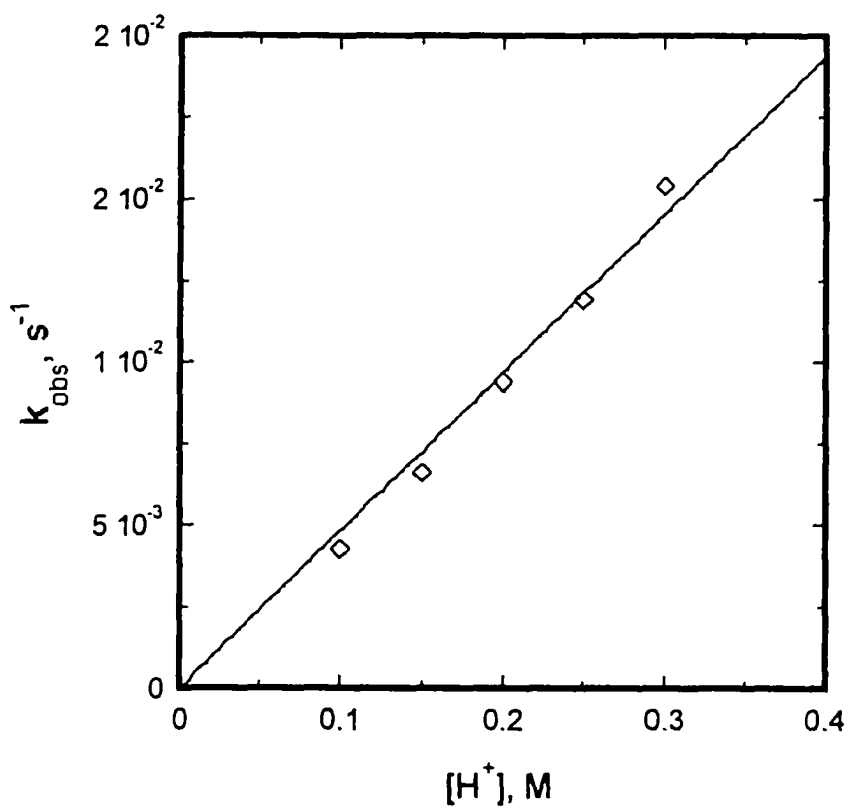
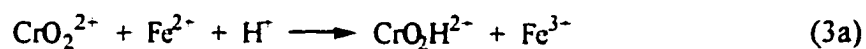


Figure 5. Acid effect on the reaction between AcrH_2 (2×10^{-4} M) and chromate (2×10^{-5} M), $[\text{H}^+] = 0.1 - 0.3$ M, $\mu = 1$, air saturated solution.

between AcrH₂ and oxygen. **Figure 6** shows a series of experiments performed with either excess of AcrH₂ or chromate, where after completion of the reaction a new aliquot of the limiting reagent was added to the reaction mixture. In the case where AcrH₂ was taken in a large excess, successive yields of AcrH⁺ were lower with each new addition of chromate and the rates were diminished. Such behavior was not observed when chromate was in excess, where the interference of AcrH₂/O₂ reaction was minimal.

In another experiment, 4×10^{-5} M chromate was allowed to react with 8×10^{-5} M AcrH₂ in an oxygen-saturated solution. The reaction was monitored at 358 nm. After the reaction was finished, 2×10^{-4} M Fe²⁺ was added to scavenge CrO₂²⁻, eq 3a,^{9c} and UV spectra were recorded every 2 minutes. The spectra were corrected for the dilution factor and for the absorbance of AcrH⁺ formed in reaction 3b.^{16a,b} The corrected spectra were subtracted from the spectrum recorded before the addition of Fe²⁺.



The resulting set of spectral changes that corresponds to the change in absorbance before and after the addition of Fe²⁺ is shown in **Figure 7**. The negative absorbance change around 290 nm suggests that a measurable amount of superoxochromium ion CrO₂²⁻ (approximately 50% of the starting amount of chromate ions) was present before addition of Fe²⁺; it then was consumed in the reaction with Fe²⁺.

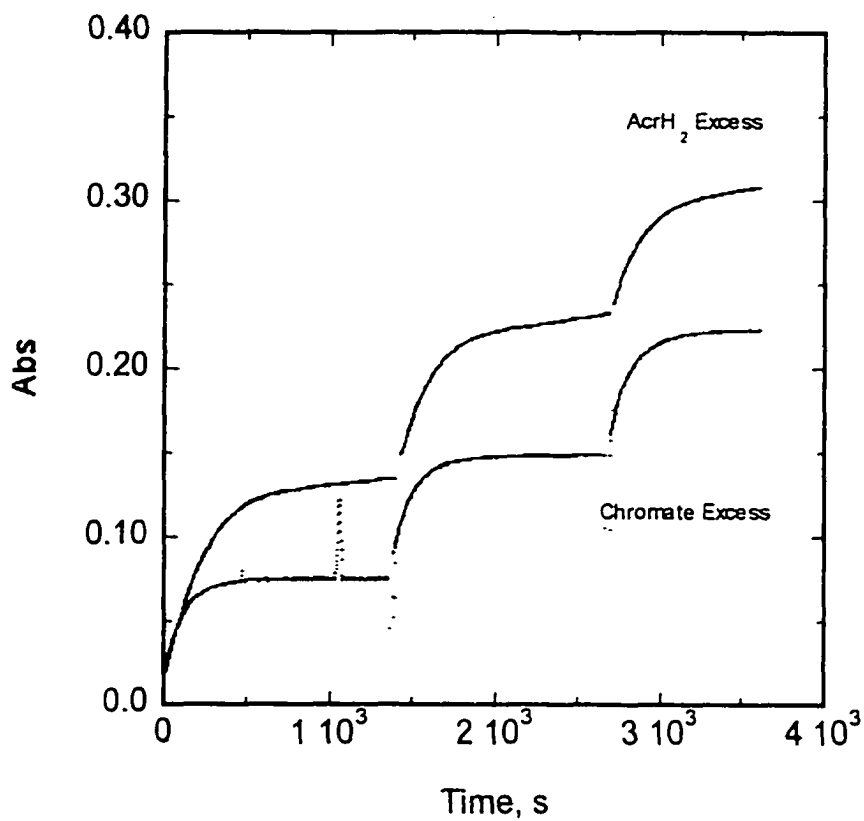


Figure 6. Reactions of a) AcrH₂ (2×10^{-5} M) with chromate (2×10^{-4} M), bottom, b) AcrH₂ (2×10^{-4} M) with chromate (2×10^{-5} M) top, pH = 1, μ = 1 M. Each aliquot of the limiting reagent was added after 20 minutes in succession.

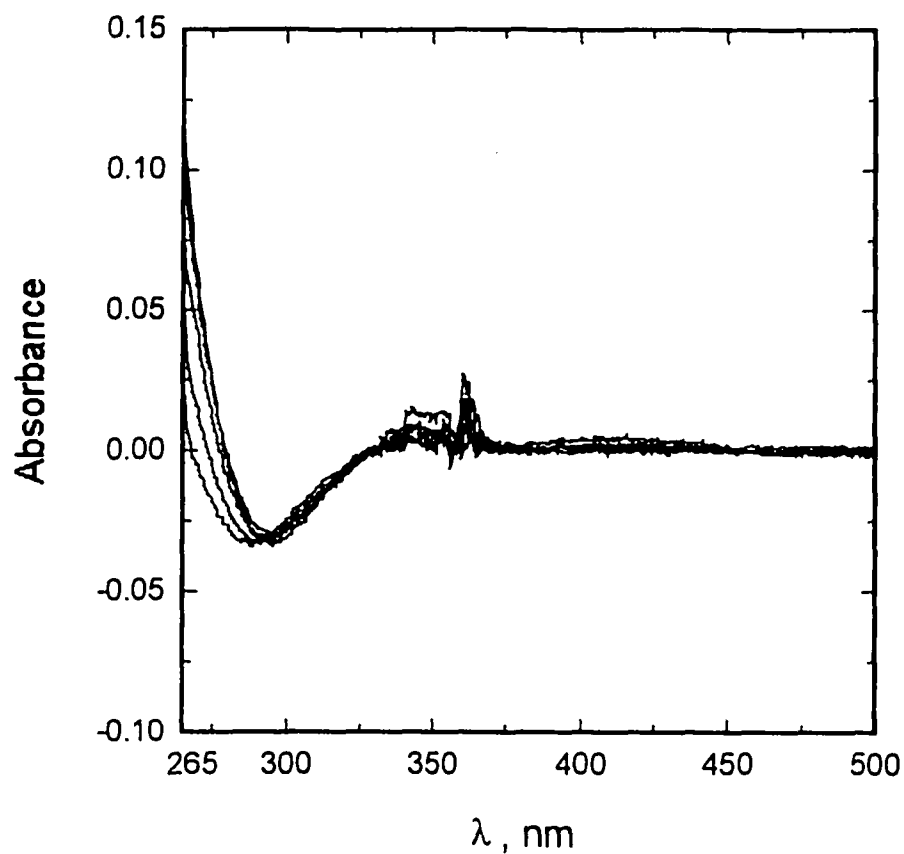


Figure 7. Reaction of AcrH_2 ($8 \times 10^{-5} \text{ M}$) with chromate ($4 \times 10^{-5} \text{ M}$) and Fe^{2+} ($2 \times 10^{-4} \text{ M}$), $\text{pH} = 1$, $\mu = 1 \text{ M}$, oxygen saturated solution. The Fe^{2+} solution was added after the reaction of chromate with AcrH_2 was complete. The spectral changes shown here represent the difference in absorbance before and immediately after the addition of Fe^{2+} .

Kinetics of the reaction between AcrH₂ and chromate under air-free conditions. This system was studied with the use of the stopped-flow technique. The reactions were monitored by following the buildup of AcrH⁺ at 358 or 417 nm. Reaction rates were significantly higher compared to those obtained with oxygen- or air-saturated solutions, ranging from a 10- to 250-fold acceleration depending on whether excess of AcrH₂ or chromate was used, respectively. In both cases, the rates obeyed pseudo-first-order kinetics. **Figures 8 and 9** show the linear dependence of the pseudo-first-order rate

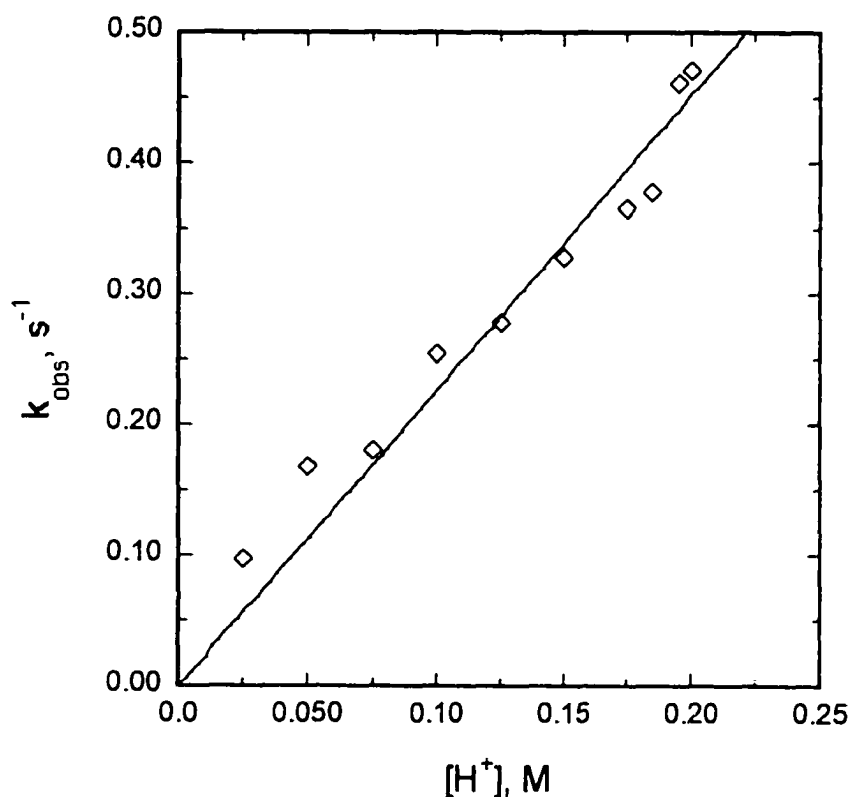


Figure 8. Acid effect on the reaction between AcrH₂ (7.5×10^{-5} M, 6.27×10^{-5} M average) and chromate (1.0×10^{-5} M), $[H^+] = 0.025 - 0.185$ M, $\mu = 1$ M, oxygen free solution.

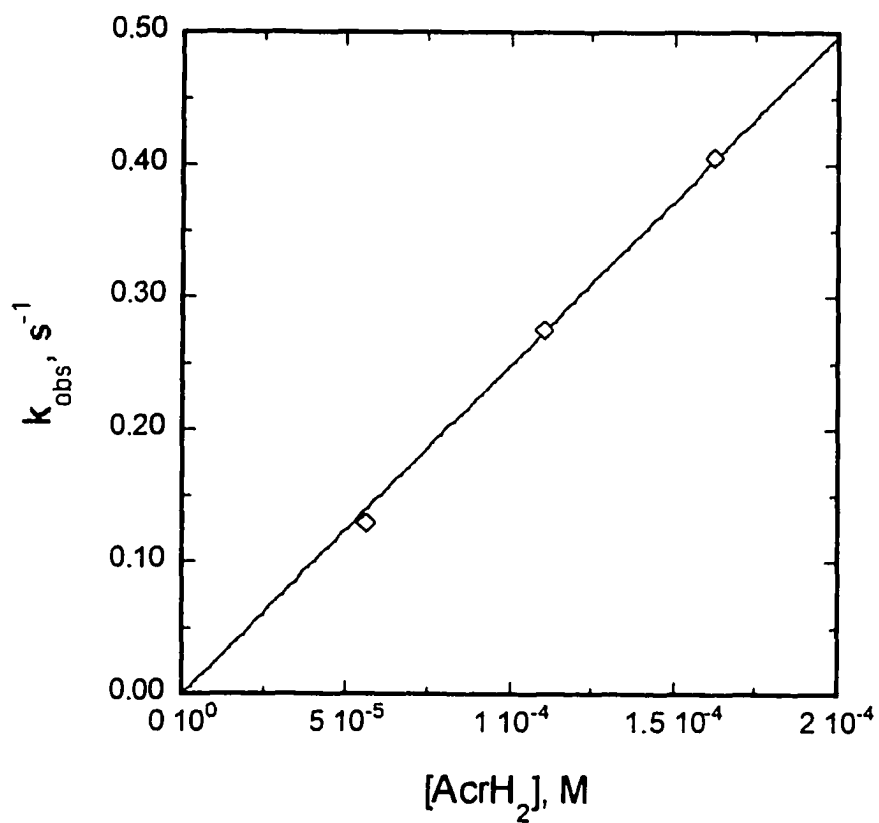


Figure 9. $[\text{AcrH}_2]$ effect on the reaction between AcrH_2 ($(5.6 - 16.2) \times 10^{-5}$ M average) and chromate (3×10^{-5} M), $\text{pH} = 1$, $\mu = 1$ M, oxygen free solution.

constants k_ψ on the acid and AcrH₂ concentrations. The fitting of data in Figures 8 and 9 to eq 4 yielded the third order rate constant $k_a = (2.49 \pm 0.04) \times 10^4 \text{ L}^2 \text{ mol}^{-2} \text{ s}^{-1}$.

$$k_\psi = k_a [\text{H}^+] [\text{AcrH}_2] \quad (4)$$

In the case of excess chromate, the values of k_ψ showed a linear dependence on the chromate concentration, **Figure 10**. The k_ψ values in Figure 10 were fitted to equation $k_\psi = k_b [\text{Cr}^{\text{VI}}]_{\text{T}}$, from which the second order rate constant is $k_b = (9.53 \pm 0.02) \times 10^1 \text{ L mol}^{-1} \text{ s}^{-1}$ (0.10 M H⁺). Saturation kinetics was observed in the [H⁺] variation experiments, as shown in **Figure 11**. The data in Figures 10 and 11 are consistent with the rate law in eq 5.

$$v = k_c / (1 + k_d [\text{H}^+]) \times [\text{H}^+] [\text{Cr}^{\text{VI}}]_{\text{T}} [\text{AcrH}_2] \quad (5)$$

The fitting yielded $k_c = (1.10 \pm 0.03) \times 10^3 \text{ L}^2 \text{ mol}^{-2} \text{ s}^{-1}$ and $k_d = 1.90 \pm 0.10 \text{ L mol}^{-1}$. No intermediates were observed upon mixing of the excess of chromate with AcrH₂ solution and taking a rapid spectral scan in the region between 300 and 700 nm.

A series of experiment with varying concentrations of sodium sulfate added to the reaction mixture with the excess of AcrH₂ was performed to study a possible formation of ion-pairs, as discussed later. No rate inhibition was observed when up to 0.05 M SO₄²⁻ was added.

Kinetic isotope effect studies. The 9,9'-dideuterated analog of AcrH₂, AcrD₂, was used (in D₂O/AN solvent mixture) to evaluate the kinetic isotope effect of the reaction between dihydroacridine and chromate. In oxygen saturated solutions, [Cr^{VI}]_T variation experiments were performed, **Figure 12**. The fitting of the experimental data to eq 2 yielded $k_{11}^{\text{D}} = (9.4 \pm 1.7) \times 10^1 \text{ L}^2 \text{ mol}^{-2} \text{ s}^{-1}$ and $k_{12}^{\text{D}} = (6.5 \pm 1.2) \times 10^3 \text{ L}^2 \text{ mol}^{-2} \text{ s}^{-1}$.

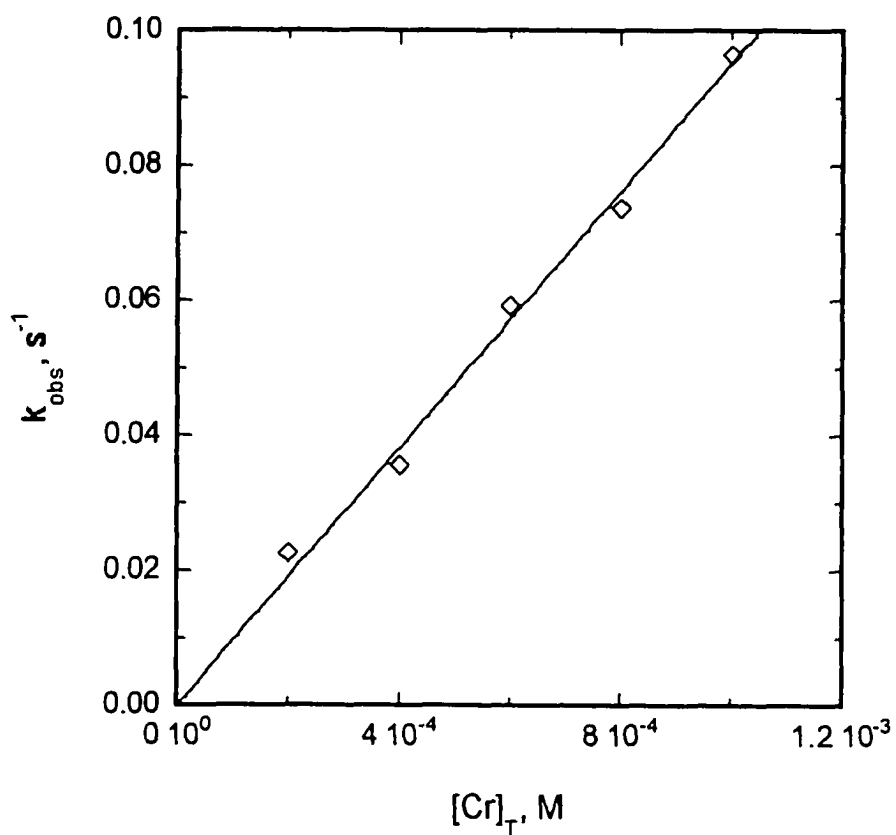


Figure 10. Chromate effect on the reaction between AcrH_2 (1.55×10^{-5} M) and chromate ($(2 - 10) \times 10^{-4}$ M), $\text{pH} = 1$, $\mu = 1$, oxygen free solution.

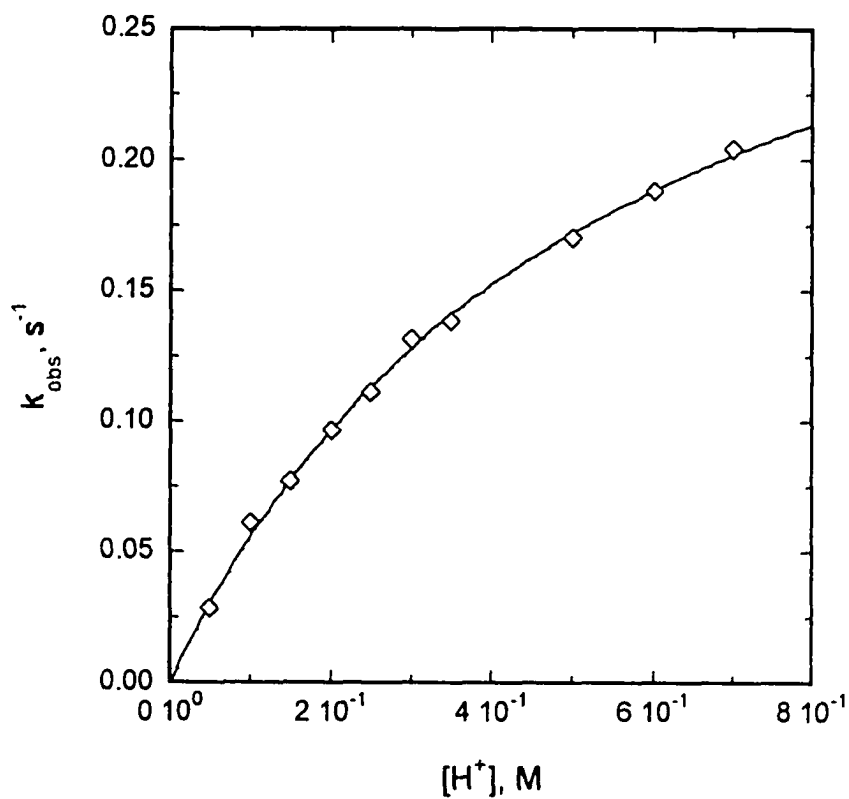


Figure 11. Acid effect on the reaction between AcrH_2 (1×10^{-5} M) and chromate (6×10^{-4} M), $[\text{H}^+] = 0.05 - 0.7$ M, $\mu = 1$ M, oxygen free solution.

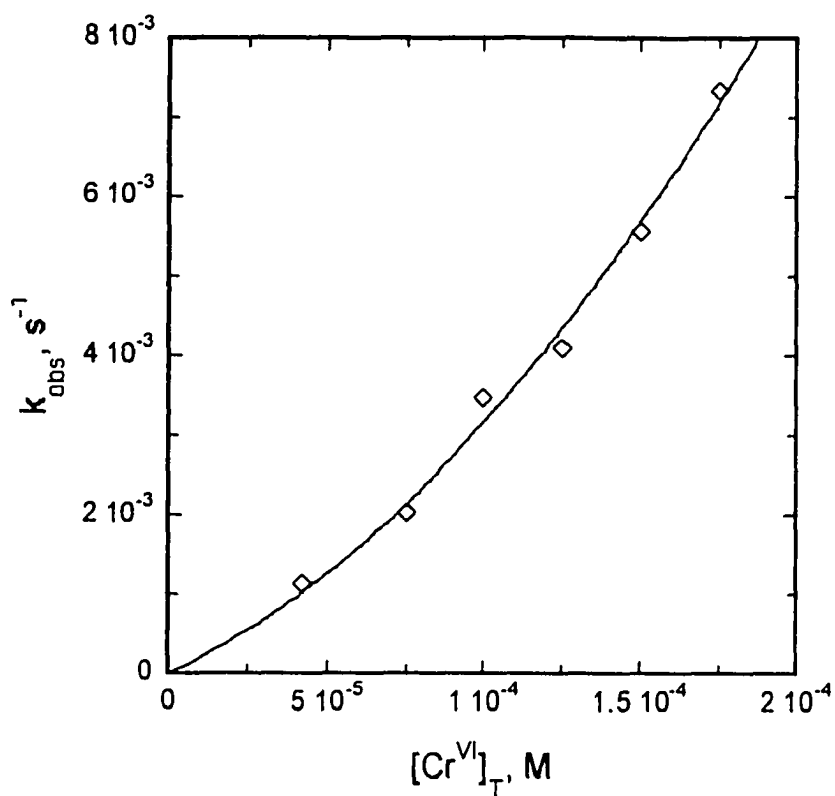


Figure 12. Chromate effect on the reaction between AcrD_2 ($2 \times 10^{-5} \text{ M}$) and chromate ($(5 - 17.5) \times 10^{-4} \text{ M}$), $\text{pH} = 1$, $\mu = 1 \text{ M}$, oxygen saturated solution.

The corresponding isotope effects are then $(k_H/k_D)_{11} = 1.2 \pm 0.2$ and $(k_H/k_D)_{12} = 0.86 \pm 0.17$.

The reaction under air-free conditions exhibited no kinetic isotope effect when an excess of chromate was used. Under the conditions with excess of AcrD_2 ($\mu = 0.10 \text{ M}$), the reaction showed a mild isotope effect of $k_H/k_D = 1.71 \pm 0.06$, **Figure 13**.

In another series of experiments the kinetic isotope effect for the reaction between chromate and AcrH_2 under anaerobic conditions was determined with the use of product ratios calculated from $^1\text{H-NMR}$ data. In a typical kinetic run, an excess of AcrD_2 ($(1 - 2) \times 10^{-4} \text{ M}$) was mixed with AcrH_2 ($(4 - 10) \times 10^{-5} \text{ M}$) and the resulting mixture was allowed to react with chromate ($2 \times 10^{-5} \text{ M}$). The reaction was followed to completion by UV-vis spectroscopy and an $^1\text{H-NMR}$ spectrum was taken. The product ratios ($[\text{AcrH}^+]_\infty/[\text{AcrD}^+]_\infty$) and the absolute concentrations were determined by analyzing the relative peak areas for the proton in position 9 (I_a) and the eight protons in positions 1 – 8 (I_b). The following formulas were used in the calculations:

$$[\text{AcrH}^+]_\infty/[\text{AcrD}^+]_\infty = 8 I_a / (I_b - 8 I_a) = R \quad (6a)$$

$$[\text{AcrH}^+]_\infty = R \Delta\text{Acr} / (R + 1) \quad (6b)$$

$$[\text{AcrD}^+]_\infty = \Delta\text{Acr} / (R + 1) \quad (6c)$$

where $\Delta\text{Acr} = 3/2 [\text{Cr}^{6+}]_0$ (since chromate is the limiting reagent, 3/2 stoichiometric coefficient was used). The kinetic isotope effect for the chain reaction $(k_H/k_D)_{\text{chain}}$ was

then calculated from eq 7.

$$(k_H/k_D)_{\text{chain}} = \frac{\ln \{ [\text{AcrH}_2]_0 / ([\text{AcrH}_2]_0 - [\text{AcrH}^+]_{\infty}) \}}{\ln \{ [\text{AcrD}_2]_0 / ([\text{AcrD}_2]_0 - [\text{AcrD}^+]_{\infty}) \}} \quad (7)$$

Due to the limited resolution of the NMR instrumentation and interference from HDO (traces of non-deuterated water were not excluded from DClO_4 stock solutions), the

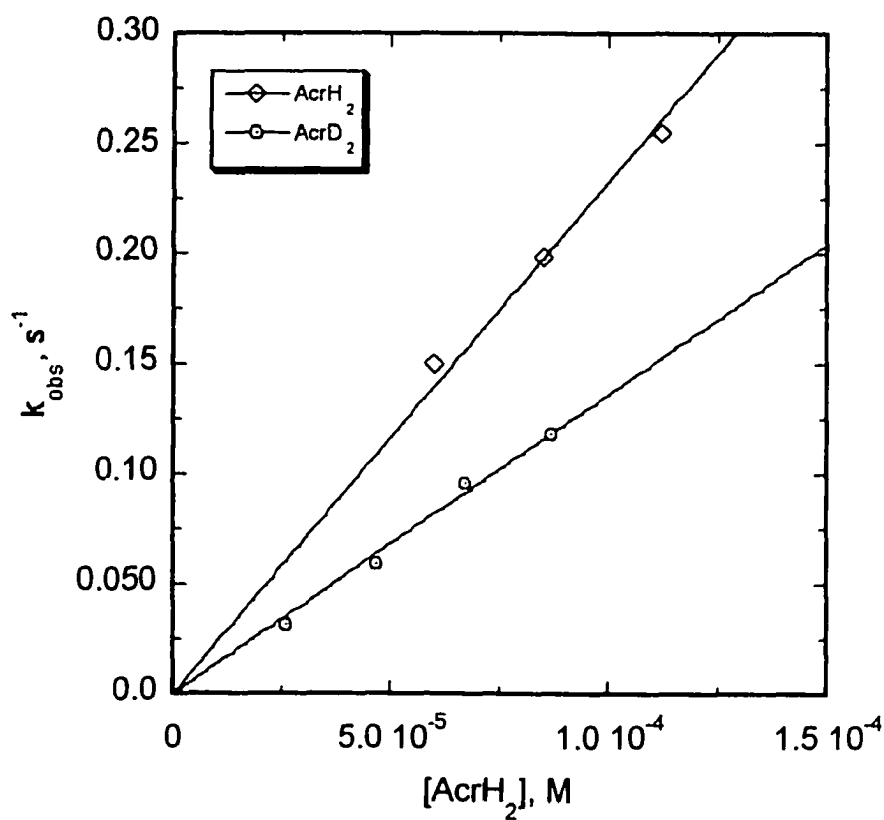


Figure 13. Reactions of AcrH_2 (in H_2O) and AcrD_2 (in D_2O) with chromate (1×10^{-5} M), $\text{pH} = 1$, $\mu = 0.1$ M, oxygen free solution.

$(k_I/k_D)_{\text{chain}}$ values have a sizable standard error, $(k_I/k_D)_{\text{chain}} = 3.0 \pm 1.1$. Isotope incorporation from the solvent into the products was not observed in the oxidation of AcrH₂ in D₂O or the oxidation of AcrD₂ in H₂O.

Reaction of chromyl ion (CrO²⁺) with AcrH₂. Chromyl ions were generated in situ by reacting 3×10^{-4} M Cr²⁺ in an oxygen-free solution with an equal volume of an air-saturated solution of AcrH₂ ($1 - 2 \times 10^{-4}$ M) in a series of stopped-flow experiments.^{9a} The concentration of chromyl ions was determined from the absorbance buildup of AcrH⁺ at 358 nm; it varied from 5 to 7×10^{-5} M. Kinetics of the reaction obeyed a second-order rate law ($\text{AcrH}_2 + \text{CrO}^{2+} + \text{H}^+ \longrightarrow \text{AcrH}^+ + \text{Cr}^{2+} + \text{H}_2\text{O}$). The second-order rate constant k_2 for the reaction between CrO²⁺ and AcrH₂ was determined from a fit of the kinetic data to eq 8, $k_2 = (1.02 \pm 0.08) \times 10^4 \text{ L mol}^{-1} \text{ s}^{-1}$.

$$[\text{AcrH}^+]_t = [\text{CrO}^{2+}]_0 \frac{\Delta_0 [\text{CrO}^{2+}]_0}{[\text{AcrH}_2]_0 e^{k \Delta_0 t} - [\text{CrO}^{2+}]_0} \quad (8)$$

where $\Delta_0 = [\text{AcrH}_2]_0 - [\text{CrO}^{2+}]_0$.

A series of experiments was carried out with methanol as a competing reagent for CrO²⁺. Methanol (0.10 M) was allowed to react with chromyl in the absence and presence of AcrH₂ (2×10^{-4} M), while keeping the experimental conditions identical. The kinetic traces from both experiments were fitted to a first-order rate law (the amount of AcrH₂ consumed under these conditions is relatively small since ~70% of chromyl ions should react with methanol). The pseudo-first-order rate constants thus obtained were 4.68 s^{-1} (0.10 M MeOH) and 6.43 s^{-1} (0.10 M MeOH, 2×10^{-4} M AcrH₂). The calculated rate

constant, $k_{\text{MeOH}} [\text{MeOH}] + k_2 [\text{AcrH}_2] = 4.68 + 2.04 = 6.72 \text{ s}^{-1}$, agrees with the measured value of 6.43 s^{-1} , and provides independent support for the value of k_2 .

In another set of experiments, chromyl ions were prepared and then diluted to approximately $1.5 \times 10^{-6} \text{ M}$. This solution of CrO^{2+} was allowed to react with $(5 - 12.5) \times 10^{-5} \text{ M}$ AcrH_2 in a conventional UV-vis spectrophotometer. **Figure 14** shows a plot of k_{ψ} against the average AcrH_2 concentration. The second-order rate constant was calculated from the slope of the plot, $k_2 = (1.10 \pm 0.06) \times 10^4 \text{ L mol}^{-1} \text{ s}^{-1}$. This value is in excellent agreement with the value obtained in the stopped-flow experiments. The reaction with AcrD_2 under the same conditions yielded $k_2^{\text{D}} = (4.8 \pm 0.2) \times 10^3 \text{ L mol}^{-1} \text{ s}^{-1}$, **Figure 15**. The kinetic isotope effect was calculated as $(k_{\text{H}}/k_{\text{D}})_2 = 2.29 \pm 0.16$.

Discussion

General observations and the reaction scheme. The experimental data described above suggest that a chain reaction operates under air-free conditions. The stoichiometry experiments provide the necessary information to deduce the final products under air-free and air-saturated conditions. Considering the fact that the only stable product formed from AcrH_2 is the acridinium ion AcrH^+ , (simulation studies with the program KinSim showed that the dimerization of the radical AcrH^{\cdot} is not important under the conditions used in this study), the final chromium-containing product under air-free conditions must be Cr^{III} . Similarly, a formal " Cr^{II} " species must be formed when significant amounts of oxygen were present during the reaction and a stoichiometric ratio $\text{AcrH}_2/\text{Cr}(\text{VI}) = 2:1$ was observed. This species is probably the superoxochromium(III)

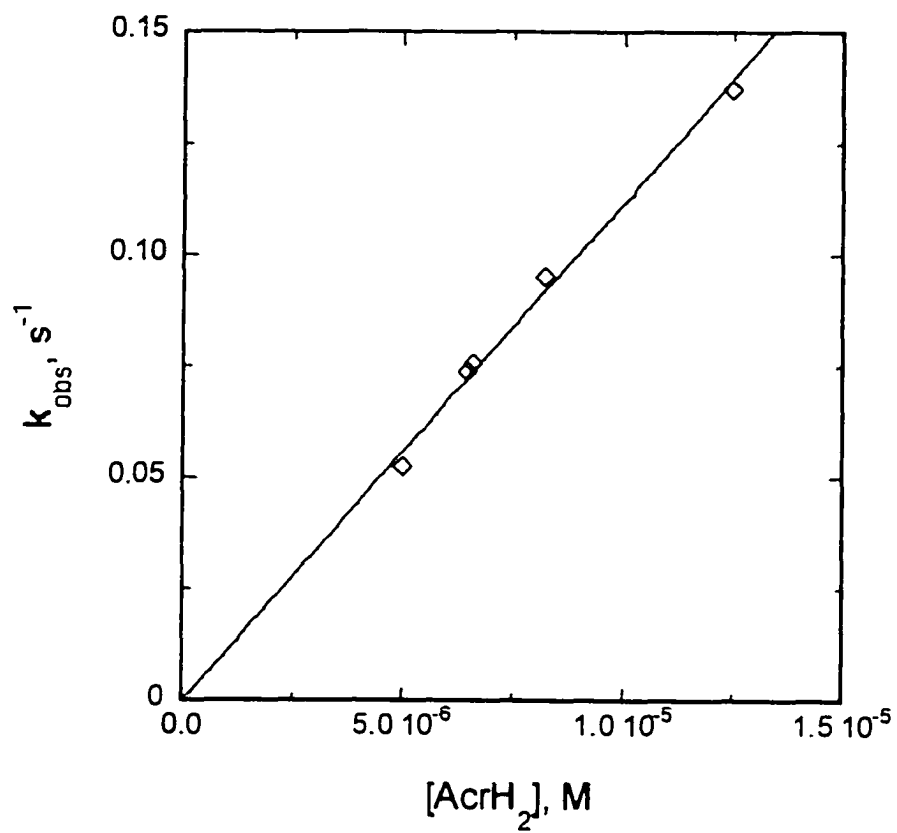


Figure 14. Reaction between CrO^{2+} ($\sim 1.5 \times 10^{-6} \text{ M}$) and AcrH_2 ($(5 - 12.5) \times 10^{-5} \text{ M}$), $\text{pH} = 1$, $m = 1 \text{ M}$, air saturated solution.

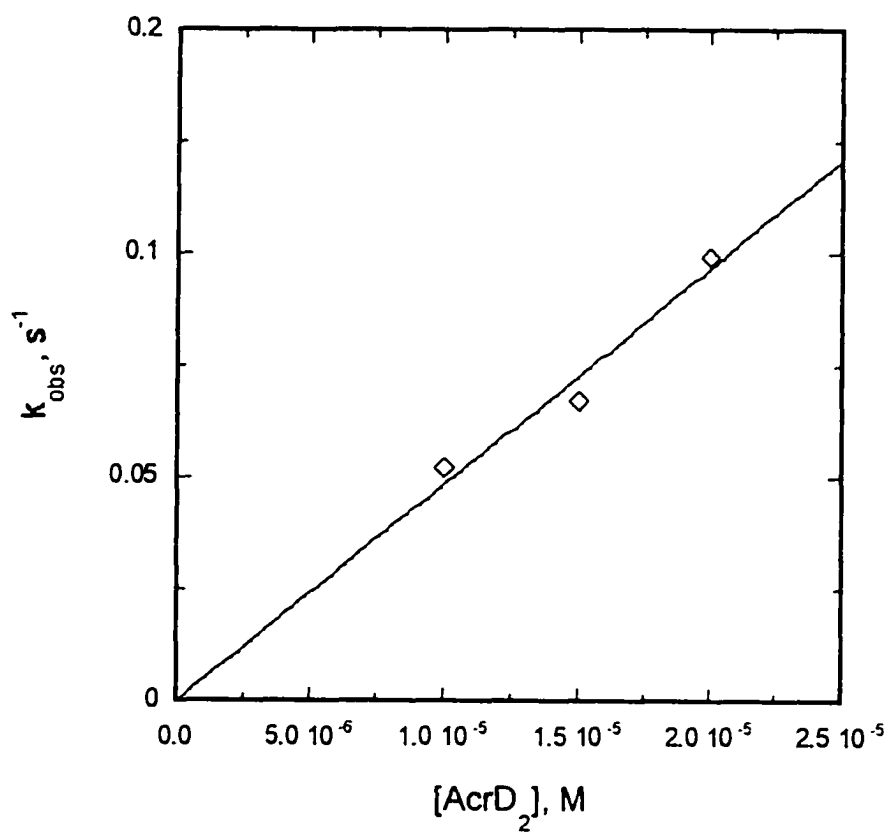
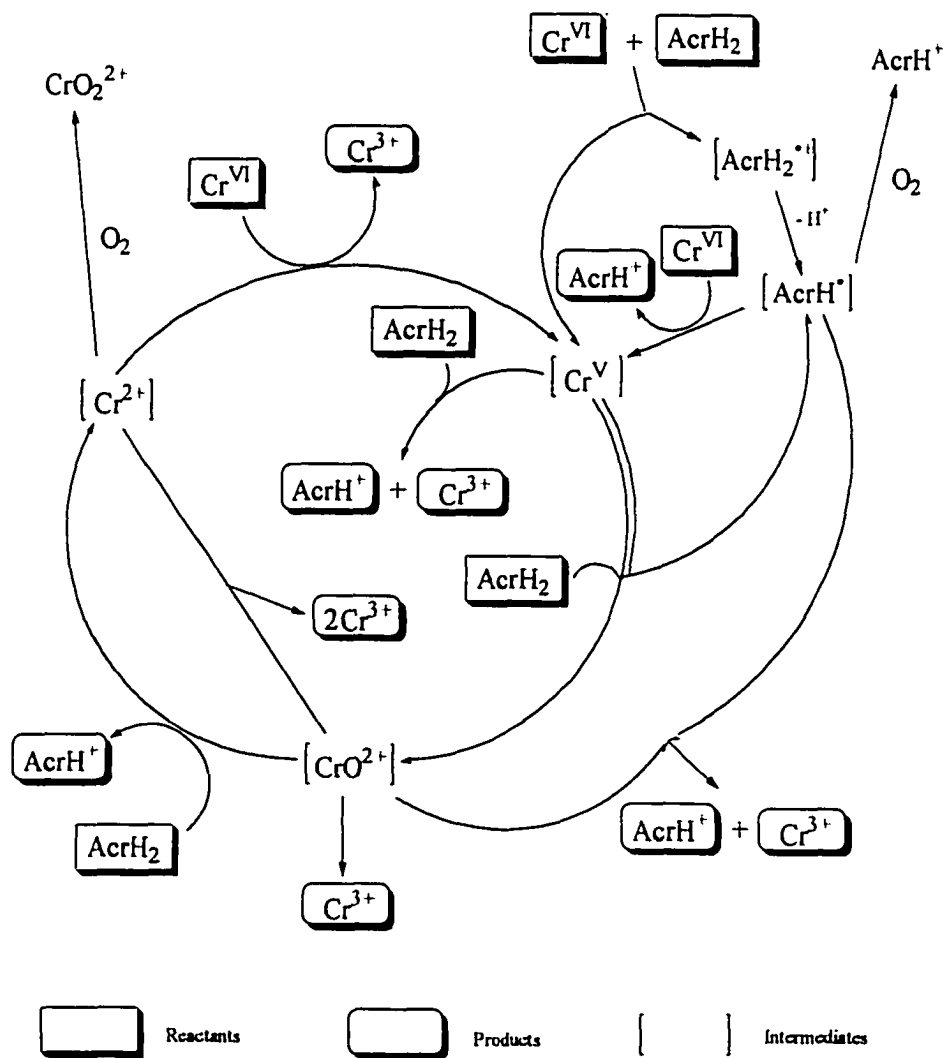


Figure 15. Reaction between AcrD_2 ($(1 - 2) \times 10^{-5} \text{ M}$) and chromyl ($\sim 1.5 \times 10^{-6} \text{ M}$), $\text{pH}=1$, $\mu = 1$, air saturated solution.

ion CrO_2^{2+} , formed in the reaction between Cr^{2+} and oxygen; its characteristic absorption at 290 nm was observed, as described in the Results section.

All the observations, including kinetics data and kinetic isotope effect experiments, are consistent with **Scheme I**. **Scheme II** shows a set of reactions with the corresponding rate constants, that were either obtained in this work or in previous studies. Also, the kinetics data are summarized in **Table I**. KinSim simulations confirmed, that under all conditions used in this study, Scheme I adequately describes the kinetic behavior of the chromate/AcrH₂ system.

Scheme I



Scheme II

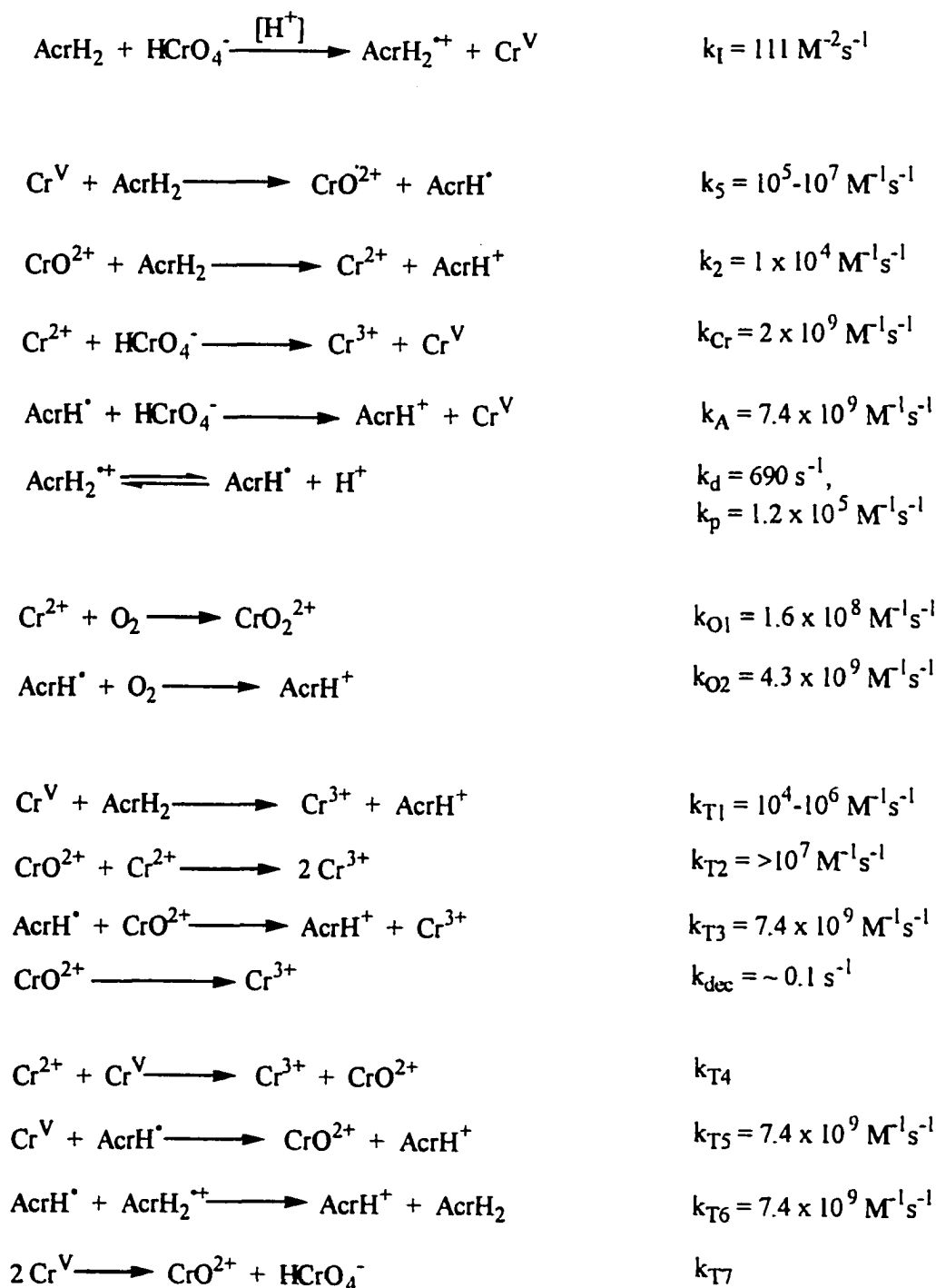


Table I. Summary of Kinetic Data for the Reactions of AcrH₂ with Chromate.

Reactants	Products	Rate constants	References
H ₂ CrO ₄ + AcrH ₂	→ Cr ^V + AcrH ₂ ^{•+}	436 ± 18	a
Cr ₂ O ₇ ²⁻ + AcrH ₂ + H ⁺	→ CrO ²⁺ + HCrO ₄ ⁻ + AcrH [•]	(6.9 ± 0.4) × 10 ³	a
Cr ^V + AcrH ₂	→ CrO ²⁺ + AcrH [•]	10 ⁵ - 10 ⁷	b,c
Cr ^V + AcrH ₂	→ Cr ³⁺ + AcrH [•]	10 ⁴ - 10 ⁶	b,c
CrO ²⁺ + AcrH ₂	→ Cr ²⁺ + AcrH [•]	(1.10 ± 0.06) × 10 ⁴	a
Cr ²⁺ + HCrO ₄ ⁻	→ Cr ³⁺ + Cr ^V	2 × 10 ⁹	9a
AcrH [•] + HCrO ₄ ⁻	→ AcrH [•] + Cr ^V	7.4 × 10 ⁹	d
AcrH ₂ ^{•+}	→ AcrH [•] + H ⁺	690	16
	←	1.2 × 10 ⁵	16
Cr ²⁺ + O ₂	→ CrO ₂ ²⁺	1.6 × 10 ⁸	21
AcrH [•] + O ₂	→ AcrH [•]	≈ 4.3 × 10 ⁹	a
CrO ²⁺ + Cr ²⁺	→ 2 Cr ³⁺	> 10 ⁷	b
AcrH [•] + CrO ²⁺	→ AcrH [•] + Cr ³⁺	7.4 × 10 ⁹	d
CrO ²⁺	→ Cr ³⁺	≈ 0.1	b

a) Obtained in this work

b) Estimated from KinSim simulations

c) See Discussion for acid effects

d) Diffusion-controlled rate constant (See ref. 5 and 20)

The initiation step in the chain reaction. The initiation step in Scheme I is the reaction between hydrogen chromate and dihydroacridine ions. The kinetics of the initiation step was studied under aerobic conditions, under which both chain cycles in Scheme I are effectively broken by the reactions of AcrH^\cdot and Cr^{2+} with oxygen. The resulting scheme is reduced to the reactions occurring prior to the reactions with oxygen, and is kinetically controlled only by the initiation step.

The reaction between AcrH^\cdot and oxygen was reported previously.^{16a} In the reaction of IrCl_6^{2-} with an excess of AcrH_2 , the stoichiometry was reduced, when air-saturated solutions were used ($[\text{IrCl}_6^{2-}] = 2 \times 10^{-4}$ M, $[\text{AcrH}_2] = 5 \times 10^{-5}$ M, stoichiometry 1.4:1 in an air-saturated solution, 1.95:1 in an air-free solution). Assuming that the rate of the reaction between AcrH^\cdot and IrCl_6^{2-} is diffusion controlled, $k = 7.4 \times 10^9$ L mol⁻¹ s⁻¹, one can estimate the rate constant for the reaction between AcrH^\cdot and oxygen as $\sim 4.3 \times 10^9$ L mol⁻¹ s⁻¹. No other products besides AcrH^\cdot were observed.

Quantitative analysis of the kinetic data for the reaction between an excess of AcrH_2 with chromate in air-saturated and oxygen-saturated solutions was difficult because of the interference from the background reaction of excess AcrH_2 with oxygen. This limitation does not apply when excess of chromate is used, hence all of the quantitative studies of the $\text{AcrH}_2/\text{Cr}^{\text{VI}}$ reaction under aerobic conditions were carried out with the excess of chromate.

A series of nonlinear least-squares fittings of the $[\text{H}^\cdot]$ and $[\text{Cr}^{\text{VI}}]_{\text{T}}$ variation data was performed to determine the elementary steps responsible for the observed kinetic behavior under aerobic conditions. The best fit occurred when both data sets were fitted

simultaneously with H_2CrO_4 and $\text{Cr}_2\text{O}_7^{2-}$ as the actual reactive species participating in electron transfers from AcrH_2 , eq 9.

$$k_{\psi} = 2 (k_{11}^e [\text{H}_2\text{CrO}_4] + k_{12}^e [\text{Cr}_2\text{O}_7^{2-}] [\text{H}^+]) \quad (9)$$

where k_{11}^e is the bimolecular rate constant for the elementary electron transfer from AcrH_2 to H_2CrO_4 , and k_{12}^e is the third-order rate constant for the electron transfer from AcrH_2 to $\text{Cr}_2\text{O}_7^{2-}$ with the assistance from H^+ .¹⁷ Overall, the latter reaction involves HCr_2O_7^- ; since its K_a is not known, a third-order rate constant notation is adopted.

Equation 9 can be rearranged to eq 10 in terms of $[\text{Cr}^{\text{VI}}]_{\text{T}}$:

$$k_{\text{obs}} = 2 \left[k_{11}^e [\text{Cr}^{\text{VI}}]_{\text{T}} \frac{[\text{H}^+]}{[\text{H}^+] + K_a} + k_{12}^e [\text{H}^+] [\text{Cr}^{\text{VI}}]_{\text{T}}^2 \frac{K_d K_a^2}{([\text{H}^+] + K_a)^2} \right] \quad (10)$$

where K_d is the dimerization constant of HCrO_4^- , and K_a the acid ionization constant of H_2CrO_4 . Using $K_d = 98 \text{ M}^{-1}$ and $K_a = 4.13$,¹⁵ k_{11}^e and k_{12}^e were determined as $436 \pm 18 \text{ L mol}^{-1} \text{ s}^{-1}$ and $(6.9 \pm 0.4) \times 10^3 \text{ L}^2 \text{ mol}^{-2} \text{ s}^{-1}$, respectively. **Figure 16** shows a plot of k_{obs} , determined in the $[\text{H}^+]$ and $[\text{Cr}^{\text{VI}}]_{\text{T}}$ variation experiments, against the values calculated from eq 10, using the rate constants obtained from the fitting. As can be seen in **Figure 16**, the agreement between the experimental and calculated k_{obs} is quite satisfactory.

The role of superoxochromim(III). As shown above, significant amounts of CrO_2^{2+} were found among products of the reaction between a small excess of AcrH_2 and chromate in air-saturated solutions. Two important conclusions can be made from these observations. First, CrO_2^{2+} does not react with AcrH_2 on the time scale of these

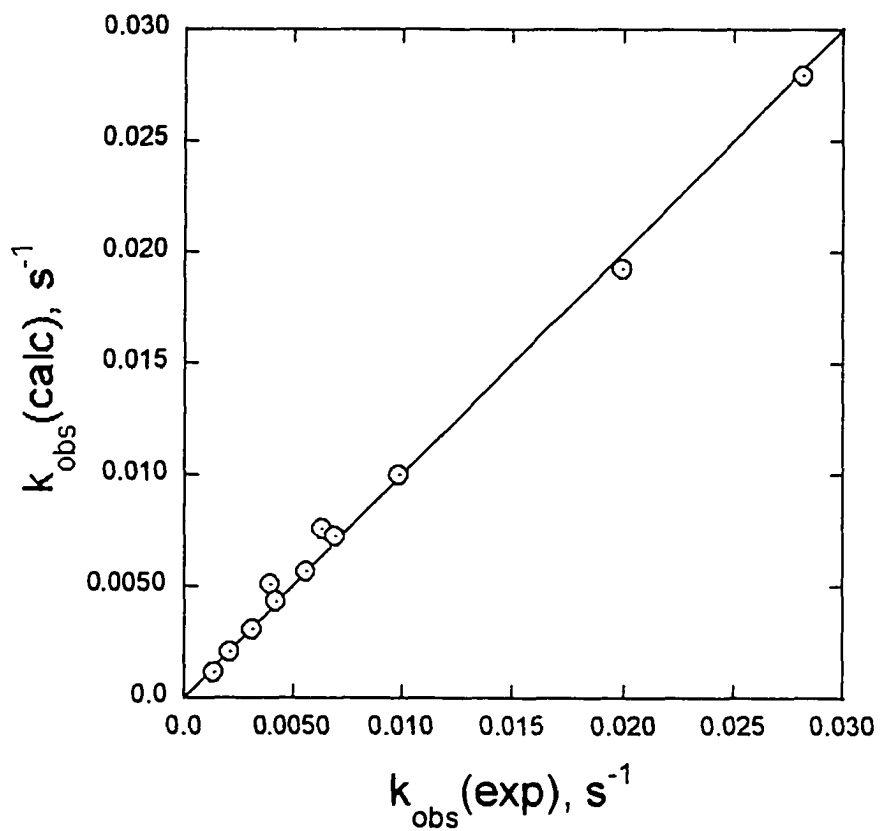
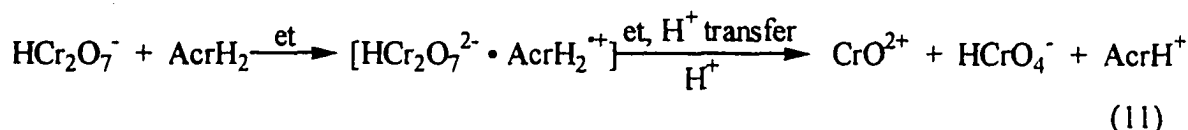


Figure 16. A comparison between the experimental and calculated values of the rate constant from the simultaneous fitting of the $[H^+]$ and $[Cr^{VI}]_T$ variation data for the reaction between excess chromate and $AcrH_2$ under aerobic conditions.

experiments (30 min to 1 hour). Second, the presence of CrO_2^{2+} indicates that Cr^{2+} is an important intermediate in the chain reaction. Since it is very unlikely that Cr^{3+} can be reduced to Cr^{2+} under these conditions, chromyl ions CrO^{2+} must also be present during the reaction.⁹ Direct studies of the reaction between chromyl and AcrH_2 showed that, indeed, CrO^{2+} ions react with AcrH_2 and produce Cr^{2+} which in turn can give CrO_2^{2+} in the reaction with oxygen. This was also confirmed by the experiments in which the AcrH^+ yields were diminished upon addition of methanol, a good trapping reagent for CrO^{2+} .

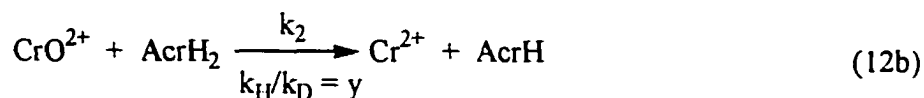
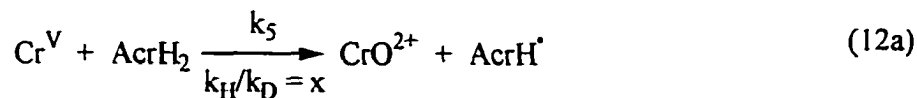
Reactions of AcrH_2 with hydrogen chromate vs. dichromate in the chain reaction. From the lack of a significant kinetic isotope effect, the reactions of AcrH_2 with hydrogen chromate and dichromate are inferred to be electron transfer processes. Although both reactions involve an initial electron transfer with the formation of Cr^{V} and $\text{AcrH}_2^{+\cdot}$ intermediates, the absence of the second-order chromate term in the rate law of the reaction between chromate and AcrH_2 under air-free conditions shows that only the reaction with hydrogen chromate ions is important as a chain initiation process. It is not clear why the reaction of dichromate with AcrH_2 is not an effective chain initiator, although one might speculate that two consecutive one-electron transfers from AcrH_2 to $\text{Cr}_2\text{O}_7^{2-}$ will produce a dimeric mixed $\text{Cr}^{\text{IV}}\text{-Cr}^{\text{VI}}$ species or a dimeric Cr^{V} intermediate, which will readily disproportionate to afford Cr^{VI} and Cr^{IV} . The second electron transfer and the required deprotonation of the acridine intermediate probably occur in a solvent cage containing an ion pair consisting of positively charged $\text{AcrH}_2^{+\cdot}$ and a double-negatively charged $\text{HCr}_2\text{O}_7^{2-}$ intermediates, eq 11.



As shown later, the Cr^{IV} intermediate (chromyl ion, CrO^{2+}) is not an efficient chain carrier under the conditions of excess chromate.

Reactions of AcrH_2 with Cr^{V} intermediates. Reactions between AcrH^{\cdot} and oxidizing reagents such as CrO^{2+} are presumed to be diffusion-controlled.^{5,18} The reaction of AcrH_2 with Cr^{V} is necessary for an effective chain reaction mechanism. Reactions T_1 , T_2 and T_3 of Scheme II are important termination steps that either control the overall propagation rate (T_1) or eliminate two chain carriers in one bimolecular process (T_2 and T_3). KinSim simulations showed that the other termination steps are unimportant under the experimental conditions used in this study. A kinetic isotope effect of 1.71 for the reaction of excess AcrH_2 with chromate under anaerobic conditions suggests that the reaction of AcrH_2 with Cr^{V} in step 5 should also have a significant isotope effect. Therefore, it is a hydrogen atom abstraction process, as opposed to an electron transfer.

A more accurate estimate of the kinetic isotope effect for the reaction between AcrH_2 and Cr^{V} can be obtained from the NMR data. The two product-forming reactions of $\text{AcrH}_2/\text{AcrD}_2$ with Cr-containing species that can distinguish between the two isotopic substrates are the reactions of Cr^{V} and CrO^{2+} (Scheme I).



Denoting the kinetic isotope effects for the two reactions in eq 12a and 12b as x and y , respectively, the overall kinetic isotope effect for the products $(k_H/k_D)_{\text{chain}}$ can be expressed in terms of x and y , eq 13a:

$$(k_H/k_D)_{\text{chain}} = \frac{2xy + x + y}{x + y + 2} \quad (13a)$$

Equation 13a can be rearranged to solve for x , eq 13b:

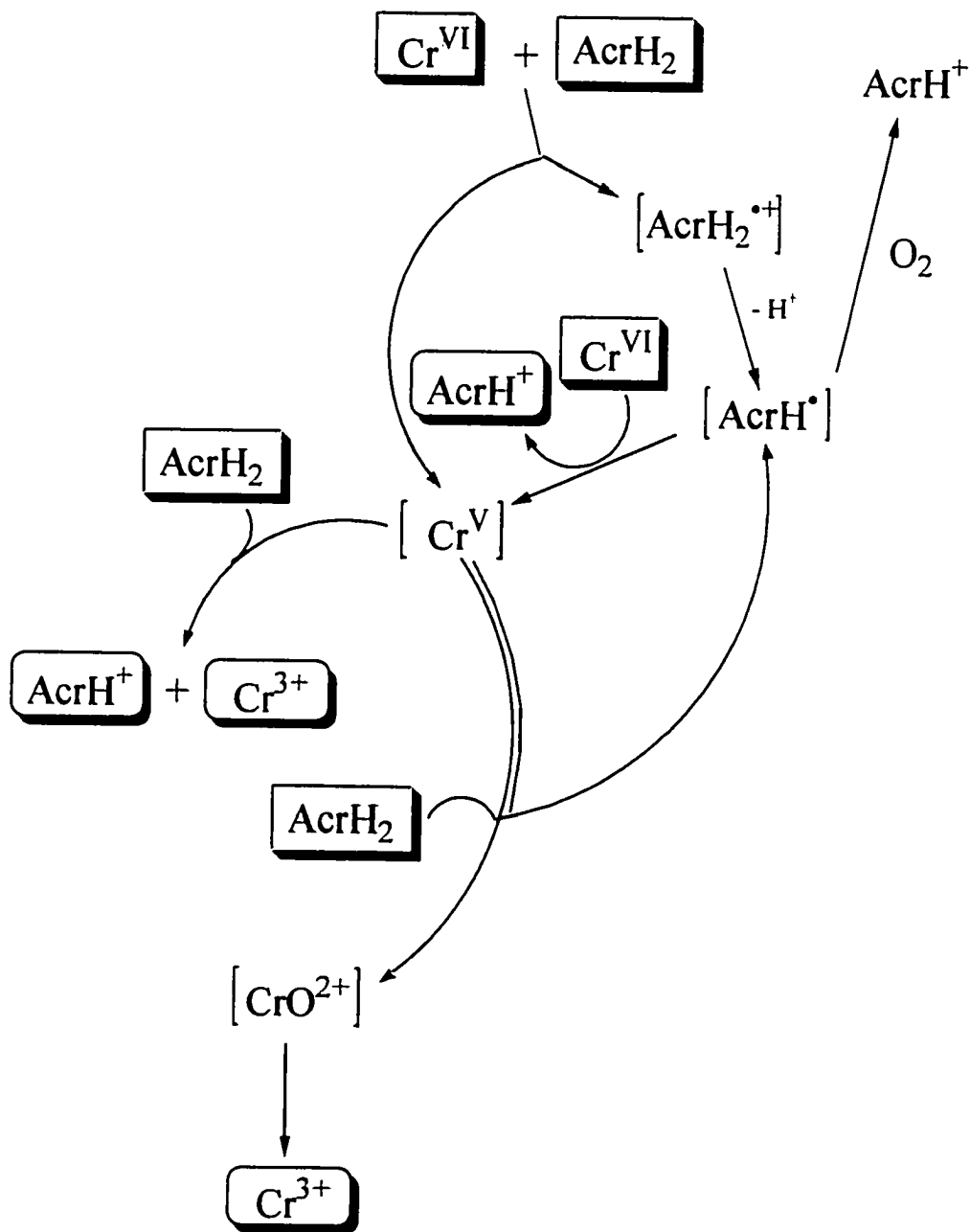
$$x = \frac{(k_H/k_D)_{\text{chain}} y + 2 (k_H/k_D)_{\text{chain}} - y}{2y + 1 - (k_H/k_D)_{\text{chain}}} \quad (13b)$$

Knowing the values of $(k_H/k_D)_{\text{chain}}$ and $(k_H/k_D)_2 = y$, the kinetic isotope effect for the reaction between AcrH_2 and Cr^{V} $(k_H/k_D)_5 = x$ can then be estimated. Due to instrumental limitations in the NMR experiments described in the Results section, the error in the value for $(k_H/k_D)_5 \approx 4.7 \pm 3.8$ is quite large. This calculation, despite the low precision, suggests, that the one-electron reaction between AcrH_2 and Cr^{V} is a hydrogen-atom abstraction process.

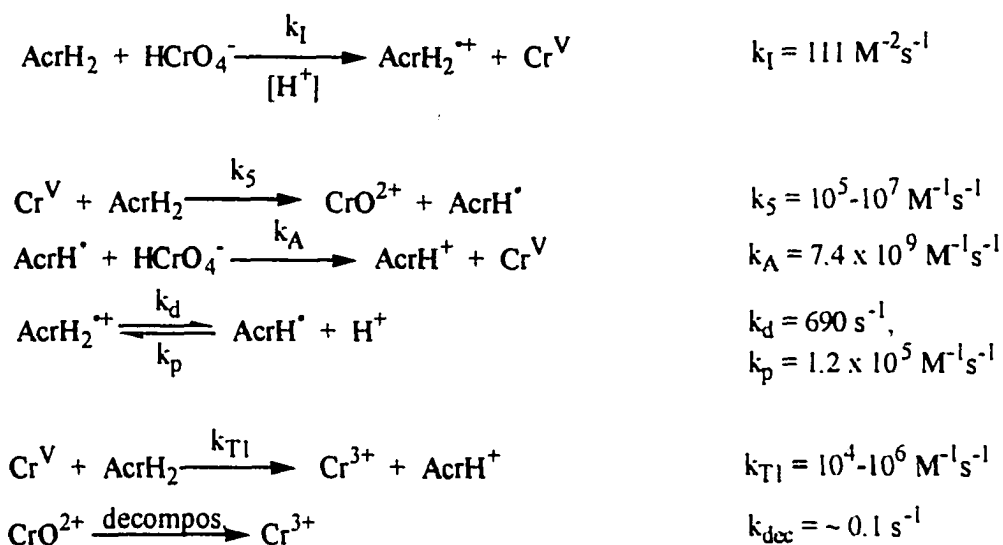
Reaction of AcrH_2 with excess chromate under anaerobic conditions. One possible explanation for the rate retardation with the change of the excess reagent involves a possibility of a chromate inhibition by forming an ion pair between hydrogen chromate and $\text{AcrH}_2^{\text{+}}$. This model is not valid, as the experiments with sodium sulfate added to the reaction mixture showed no change in the reaction rates.

Kinetic data for the reaction between AcrH_2 and excess chromate suggest that the second cycle involving a Cr^{2+} intermediate (Scheme I) is not operating under these conditions. **Schemes III and IV** show the important reactions in this system.

Scheme III



Scheme IV



Under the conditions where an excess of chromate ion was used, the competing decomposition of the chromyl ions is much faster than the propagation step 2 (Scheme II). As a result, the cycle involving the reactions of AcrH₂ with chromyl ion, and of Cr²⁺ with Cr^{VI}, is not important. Further proof of the validity of this scheme was obtained when methanol (0.01 – 0.10 M) was introduced into the reaction mixture prior to the addition of chromate. The reaction that followed was much faster than without methanol, resembling the kinetics of the AcrH₂/chromate reaction with excess AcrH₂, except that the yields of AcrH⁺ were diminished. In this experiment, methanol was added to promote the formation of Cr²⁺ from CrO²⁺ without the formation of AcrH⁺.

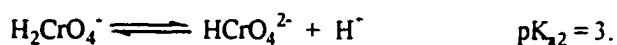
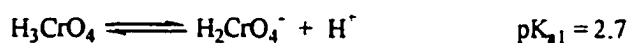
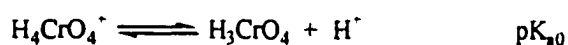
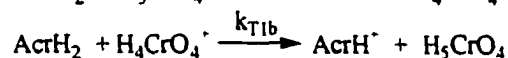
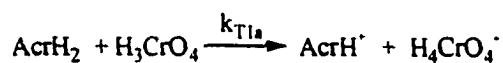
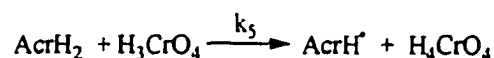
Equation 14 shows the steady-state rate law that can be derived from Scheme IV.

$$v = 2 \frac{k_I' k_5}{k_{\text{T1}}} [\text{AcrH}_2] [\text{Cr}^{\text{VI}}]_{\text{T}} \quad (14)$$

Disregarding any acid effects for now and using $k_1' = k_1 [H^+] = 11.1 \text{ L mol}^{-1} \text{ s}^{-1}$ (0.10 M H^+), the chain length can be calculated as $k_5/k_{T1} = 4.3$. The low value of k_5/k_{T1} shows that the chain reaction under these conditions is not efficient, consistent with only ~ 10-fold rate acceleration compared to the reaction carried out under aerobic conditions.

Acid effect on the reaction between AcrH₂ and excess chromate under anaerobic conditions. As described in the Results section, saturation kinetics were observed for the acid effect on the reaction between AcrH₂ and an excess of chromate. The elementary reaction steps consistent with such kinetic behavior are shown in **Scheme V**.

Scheme V



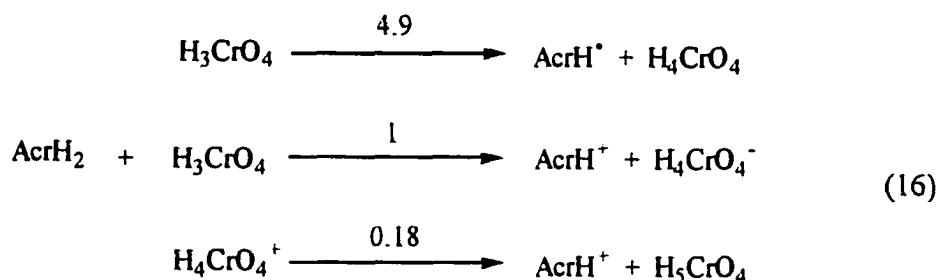
where k_5 , k_{T1a} and k_{T1b} are the second-order rate constant for the elementary reactions between Cr^V and AcrH₂ in both 1e and 2e reactions; K_{a1} , K_{a2} and K_{a3} are the acid ionization constants for various Cr^V species known to be present in aqueous solution¹⁹; K_{a0} is the acid ionization constant for the uncharacterized tetraprotonated Cr^V species. The existence of H_4CrO_4^- is a speculation, but is necessary to account for the experimentally observed rate law. Furthermore, it is reasonable to assume that H_4CrO_4^-

is a stronger 2-e oxidant than H_3CrO_4 for the process in which a formal hydride transfer occurs, because of the positive charge of the former.

The overall rate law of the chain reaction can then be expressed as in eq 15, accounting for the acid affect.

$$v = 2 k_1 k_5 \frac{K_{a0}}{k_{T1b}} \frac{[\text{H}^+]}{k_{T1a} \frac{K_{a0}}{k_{T1b}} + [\text{H}^+]} [\text{AcrH}_2] [\text{Cr}^{\text{VI}}] \quad (15)$$

In the derivation above, the following assumptions were made: a) $[\text{H}_3\text{CrO}_4] \approx [\text{Cr}^{\text{V}}]_{\text{T}}$, total concentration of Cr^{V} intermediates, and b) $[\text{H}_4\text{CrO}_4^-] \approx [\text{H}^+]/K_{a0} \times [\text{Cr}^{\text{V}}]_{\text{T}}$. Both are justified considering the values of $\text{p}K_a$ for different Cr^{V} intermediates and assuming that $K_{a0} \gg [\text{H}^+]$ under the experimental conditions used (protonation of the triprotonated Cr^{V} species occurs only to a small degree, consistent with the fact that such a species has not been observed experimentally).¹⁹ From the experimental data the ratios $k_5/k_{T1a} = 4.9$ and $k_{T1a}/k_{T1b} \times K_{a0} = 0.54$ were calculated, which allow to determine the partitioning of the different Cr^{V} species reacting with AcrH_2 at $[\text{H}^+] = 0.1 \text{ M}$, eq 16.



Conclusions

The reaction between AcrH_2 and chromate was found to be a branching chain reaction, in which transient Cr^{V} , Cr^{IV} , Cr^{II} and $\text{AcrH}^+/\text{AcrH}_2^{2+}$ species are the chain carriers. Under aerobic conditions, both chain cycles are broken by the reactions of Cr^{2+}

and AcrH^\cdot with oxygen and the rate of the overall reaction is controlled solely by the initiation step. Kinetic evidence suggests that the initiation step are the reactions of AcrH_2 with the chromic acid H_2CrO_4 and hydrogen dichromate HCr_2O_7^- which occur by an electron transfer pathway. Kinetic data and kinetic isotope effect studies provide useful information about the properties and reactivities of the transient chromium intermediates.

Acknowledgement

This work was supported by a grant from the National Science Foundation (CHE-9007283). Some experiments were conducted with the use of the facilities of the Ames Laboratory. We wish to thank Dr. Matthew Eager for valuable discussions concerning the chain reaction mechanism.

References

- (40) (a) Eisner, U.; Kuthan, J. *Chem. Rev.* **1972**, *72*, 1. (b) Stout, D. M.; Mayer, A. I. *Ibid.* **1982**, *82*, 223. (c) Shinkai, S.; Bruice, T. *Biochemistry* **1973**, *12*, 1750. (d) Kurz, L.; Frieden, C. *J. Am. Chem. Soc.* **1975**, *97*, 667. (e) Jones, J.; Taylor, K. *Can. J. Chem.* **1976**, *54*, 2974.
- (41) (a) Ohnishi, Y.; Ohno, A. *Chem. Lett.* **1976**, 697. (b) Kill, R.; Widdowson, D. *J. Chem. Soc., Chem. Commun.* **1976**, 697. (c) van Eikeren, P.; Grier, D. *J. Am. Chem. Soc.* **1977**, *99*, 8057. (d) Hajdu, J.; Sigman, D. *Ibid.* **1976**, *98*, 6060. (e) Schmakel, C.; Santhanathan, K.; Elving, P. *J. Electrochem. Soc.* **1974**, *121*, 345.

- (42) (a) van Eikeren, P.; Grier, D. L.; Eliason, J. *J. Am. Chem. Soc.* **1979**, *101*, 7406.
(b) Kim, C. S. Y.; Chaykin, S. *Biochemistry* **1968**, *7*, 2339. (c) Fukuzumi, S.;
Ishikawa, M.; Tanaka, T. *Tetrahedron* **1986**, *42*, 1021.
- (43) (a) Fukuzumi, S. In *Advances in Electron Transfer Chemistry*; Mariano, P. S.,
Ed.; JAI Press: Greenwich, 1992; Vol. 2, p 65. (b) van Eikeren, P.; Grier, D. L. *J. Am.*
Chem. Soc. **1976**, *98*, 4655. (c) Fukuzumi, S.; Kuroda, S.; Goto, T.; Ishikawa, K.;
Tanaka, T. *J. Chem. Soc., Perkin Trans. II* **1989**, 1047. (d) Fukuzumi, S.; Ishikawa,
M.; Tanaka, T. *J. Chem. Soc., Perkin Trans.* **1989**, 1037. (e) Ishikawa, K.; Fukuzumi,
S.; Goto, T.; Tanaka, T. *J. Am. Chem. Soc.* **1990**, *112*, 1577. (f) Fukuzumi, S.; Chiba,
M.; Tanaka, T. *Chem. Lett.* **1989**, 31. (g) Fukuzumi, S.; Mochizuki, S.; Tanaka, T. *J.*
Am. Chem. Soc. **1989**, *111*, 1497. (h) Fukuzumi, S.; Mochizuki, S.; Tanaka, T. *Inorg.*
Chem. **1990**, *29*, 653. (i) Fukuzumi, S.; Tokuda, Y. *J. Phys. Chem.* **1993**, *97*, 3737.
- (44) Fukuzumi, S.; Tokuda, Y.; Kitano, T.; Okamoto, T.; Otera, J. *J. Am. Chem. Soc.*
1993, *115*, 8960.
- (45) (a) Kosower, E. M. In *Free Radicals in Biology*; Pryor, W. A., Ed.; Academic
Press: New York, 1976; Vol. II, p 1. (b) Kill, R. J.; Widdowson, D. A. In *Bioorganic*
Chemistry; van Tamelen, E. E., Ed.; Academic Press: New York, 1978; Vol. IV, p
239. (c) Bruice, T. C. In *Progress in Bioinorganic Chemistry*; Kaiser, F. T., Kezdy, F.
J., Eds.; Wiley: New York, 1976; Vol. IV, p 1. (d) Yasui, S.; Ohno, A. *Bioorg. Chem.*
1986, *14*, 70.
- (46) (a) Cainelli, G.; Cardillo, G. In *Chromium Oxidations in Organic Chemistry*;
Springer-Verlag: New York, 1984; pp. 118-216 (b) Westheimer, F.H. *Chem. Rev.*
1949, *45*, 419 (c) Rocek, J.; Radkowsky, A.E. *J. Am. Chem. Soc.* **1973**, *95*, 7123 (d)
-

- Rahman, M.; Rocek, J. *J. Am. Chem. Soc.* **1971**, *93*, 5455, 5462 (e) Nag, K.; Bose, S. *N. Str. Bonding* **1985**, *63*, 153 (f) Farrel, R. P.; Lay, P. A. *Comments Inorg. Chem.* **1992**, *13*, 133 (g) Gould, E. S. *Acc. Chem. Res.* **1986**, *19*, 66 (h) Bakac, A. *Prog. Inorg. Chem.* **1995**, *43*, 267 (i) Lippard, S. J.; Berg, J. M. *Principles of Bioinorganic Chemistry* **1994**, University Science Books, Chapter 5.
- (47) (a) Rossi, S. C.; Gorman, N.; Wetterhahn, K. E. *Chem. Res. Toxicol.* **1988**, *1*, 101 (b) Goodgame, D. M. L.; Joy, A. M. *J. Inorg. Biochem.* **1986**, *26*, 219 (c) Farrel, R. P.; Judd, R. J.; Lay, P. A.; Dixon, N. E.; Baker, R. S. U.; Bohin, A. M. *Chem. Res. Toxicol.* **1989**, *2*, 227.
- (48) (a) Scott, S. L.; Bakac, A.; Espenson, J. H. *J. Am. Chem. Soc.* **1992**, *114*, 4205 (b) Al-Ajlouni, A. M.; Espenson, J. H.; Bakac, A. *Inorg. Chem.* **1993**, *32*, 3162 (c) Brynildson, M. E.; Bakac, A.; Espenson, J. H. *Inorg. Chem.* **1988**, *27*, 2592 (d) Ilan, Y. A.; Czapski, G.; Ardon, M. *Isr. J. Chem.* **1975**, *13*, 15 (e) Sellers, R. M.; Simic, M. G. *J. Am. Chem. Soc.* **1976**, *98*, 6145.
- (49) Bakac, A.; Wang, W.-D. *J. Am. Chem. Soc.* **1996**, *118*, 10325.
- (50) (a) Krumpolc, M.; Rocek, J. *J. Am. Chem. Soc.* **1979**, *101*, 3206 (b) Srinivasan, K.; Kochi, J. K. *Inorg. Chem.* **1985**, *24*, 4670 (c) Ghosh, M. C.; Gould, E. S. *J. Am. Chem. Soc.* **1993**, *115*, 3167 (d) Sugden, K. D.; Wetterhahn, K. E. *Inorg. Chem.* **1996**, *35*, 651 (e) Collins, T. J.; Slebodnick, C.; Uffelman, E. S. *Inorg. Chem.* **1990**, *29*, 3433 (f) Siddall, T. L.; Miyaura, N.; Huffman, J. C.; Kochi, J. K. *J. Chem. Soc. Chem. Commun.* **1983**, 1185 (g) Yuan, L.-C.; Bruice, T. C. *J. Am. Chem. Soc.* **1985**, *107*, 512 (h) Mitewa, M.; Russev, P.; Bontchev, P. R.; Kabassanov, K.; Malinovski, A. *Inorg. Chim. Acta* **1983**, *70*, 179 (i) Gould, E. S. *Acc. Chem. Res.* **1986**, *19*, 66 (j)

- Bakac, A. *Progress in Inorganic Chemistry*; Karlin, K. D., Ed.; Wiley: New York, 1995; Vol. 43, p 267.
- (51) Powell, M. F.; Wu, J. G.; Bruice, T. C. *J. Am. Chem. Soc.* **1984**, *106*, 3850.
- (52) Karrer, P.; Szabo, L.; Krishna, H. Y. V.; Schwyzer, R. *Helv. Chim. Acta* **1950**, *XXXIII*, 294.
- (53) Fukuzumi, S.; Koumitsu, S.; Hironaka, K.; Tanaka, T. *J. Am. Chem. Soc.* **1987**, *109*, 305.
- (54) Tong, J. Y. *Inorg. Chem.* **1964**, *3*, 1804.
- (55) (a) Pestovsky, O.; Bakac, A.; Espenson, J. H. *Inorg. Chem.* **1998**, *37*, 1616 (b) A small excess of AcrH₂ (< 5 %) was present in the reaction mixture. The kinetics of the reaction between AcrH₂ and Fe³⁺ matched those reported previously (see ref. 16a). The correction for the reaction 3b was performed by assaying the excess AcrH₂ from the absorbance of the product AcrH⁺ at 358 nm, generated during the reaction with Fe³⁺. The spectral difference for the reaction 3b, $C_{\text{AcrH}_2} \times [\epsilon_{358}(\text{AcrH}^+) + 2\epsilon_{358}(\text{Fe}^{2+}) - \epsilon_{358}(\text{AcrH}_2) - 2\epsilon_{358}(\text{Fe}^{3+})]$, was obtained from authentic samples of the corresponding reagents and was used to correct the spectral changes.
- (56) The elementary reaction between dichromate and AcrH₂ probably occurs through an initial protonation of dichromate and the formation of HCr₂O₇⁻. Since the value of the equilibrium constant for the acid ionization of HCr₂O₇⁻ is unknown, the third-order rate constant is reported for the reaction between AcrH₂ and Cr₂O₇²⁻.
- (57) Hapiot, P.; Moiroux, J.; Saveant, J.-M. *J. Am. Chem. Soc.* **1990**, *112*, 1337.
- (58) Buxton, G. V.; Djouider, F. *J. Chem. Soc., Faraday Trans.* **1996**, *92*, 4173.

- (59) Espenson, J. H. In *Chemical Kinetics and Reaction Mechanisms*; McGraw-Hill: New York, 1995; p 201.
- (60) Brynildson, M. E.; Bakac, A.; Espenson, J. H. *J. Am. Chem. Soc.* **1987**, *109*, 4579.
-

GENERAL CONCLUSIONS

Mechanisms of the reactions of 10-methyl-9,10-dihydroacridine with inorganic oxidizing reagent follow the same general scheme, Scheme V of Chapter I, in which an initial 1e oxidation of AcrH₂ produces the acridinium radical-cation AcrH₂^{•+}. The following deprotonation of the radical-cation and the sequential oxidation of thus formed acridinium radical AcrH[•] complete the 2e oxidation of AcrH₂, resulting in a formal hydride transfer from AcrH₂. Depending on the strength of the inorganic oxidant, the initial electron transfer or the following deprotonation of the radical-cation may be rate controlling. In the case of weak oxidizing reagents such as Fe_{aq}³⁺ or chromate(VI), the first electron transfer is rate-controlling and can be studied directly (the following reactions are much faster). The data from the kinetic isotope effect experiments suggest that the first 1e oxidation process is an electron transfer.

When strong oxidizing reagent with high standard oxidation potentials (Ce_{aq}⁴⁺) or fast self-exchange electron transfer rates (IrCl₆²⁻) are used, the initial electron transfer is fast and cannot be observed on the stopped-flow time scale. As a result, the properties of AcrH₂^{•+} can be studied directly, since it persists on the stopped-flow time scale. The pK_a of AcrH₂^{•+} was determined in 20% AN / 80% H₂O mixed solvent. Kinetic isotope experiments employing AcrD₂ instead of the proteo analog provide important information on intrinsic details of deprotonation of the radical-cation. Both ionization of AcrH₂^{•+} and protonation of AcrH[•] have contribution of nuclear tunneling when H[•] is transferred.

The reaction of AcrH_2 with chromate(VI) was found to be a branching chain reaction that is strongly inhibited by O_2 . An electron transfer from AcrH_2 to H_2CrO_4 is the initiation step of the chain reaction; it produces AcrH^\bullet (through an initial formation and the sequential deprotonation of the radical-cation) and Cr^{V} intermediates that are the chain carriers. $\text{Cr}_2\text{O}_7^{2-}$ reacts with AcrH_2 but does not produce any chain-carrying intermediates when excess chromate is used. This finding is consistent with the formation of CrO^{2+} in 2e oxidation of AcrH_2 by dichromate: $\text{AcrH}_2 + \text{Cr}_2\text{O}_7^{2-} \rightarrow \text{AcrH}^\bullet + \text{Cr}^{\text{VI}} + \text{CrO}^{2+}$.

A reaction between Cr^{V} and AcrH_2 can occur by either hydrogen atom abstraction of a formal hydride transfer. The former produces AcrH^\bullet and CrO^{2+} , two chain-carrying intermediates, resulting in branching. Both chain branches, involving either $\text{Cr}^{\text{V}}/\text{AcrH}^\bullet$ or $\text{Cr}^{\text{V}}/\text{CrO}^{2+}/\text{Cr}^{2+}$ intermediates are efficiently terminated in the presence of oxygen by the reactions of AcrH^\bullet and Cr^{2+} with O_2 , respectively.

A competitive hydride transfer from AcrH_2 to Cr^{V} produces AcrH^\bullet and Cr^{3+} thus resulting in an efficient chain termination. Acid effect studies suggest that a previously undetected intermediate H_4CrO_4^+ reacts with AcrH_2 by hydride transfer mechanism, competing with the reaction of H_3CrO_4 with AcrH_2 in the chain termination process. The kinetics data provide necessary information to determine the relative rates at which these competitive reactions occur at different pH.

The reaction between AcrH_2 and CrO^{2+} proceeds by a hydride transfer, which was proven by kinetic isotope effect experiments and competition with MeOH studies.

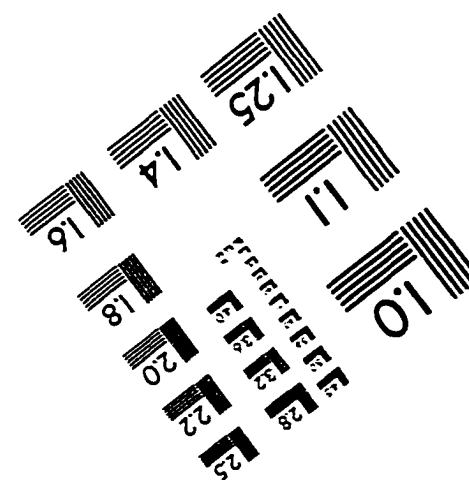
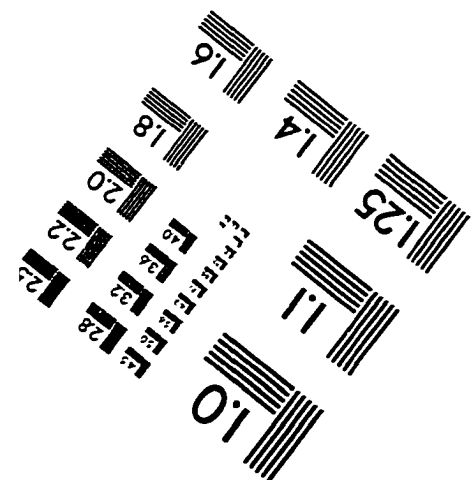
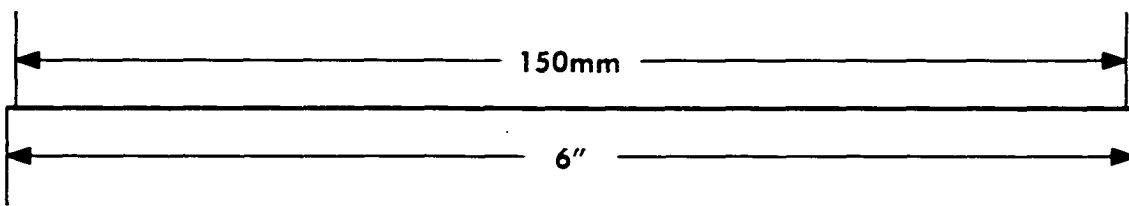
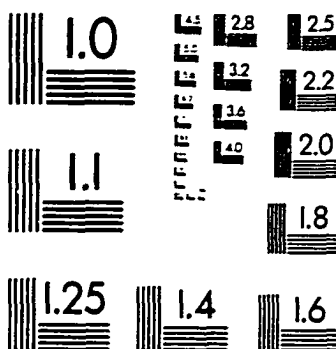
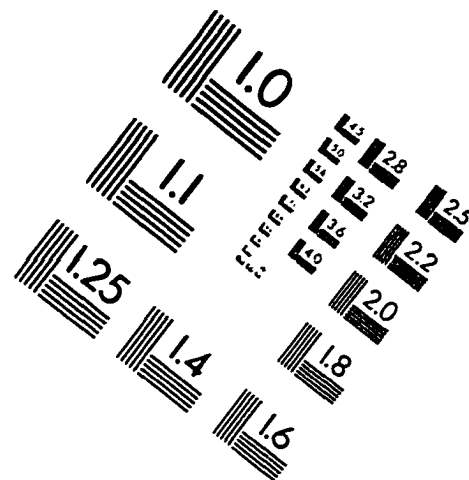
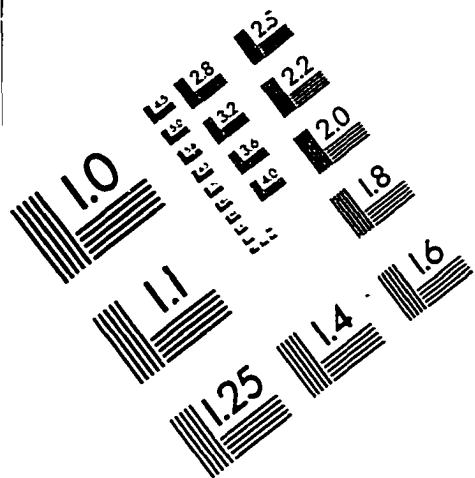
ACKNOWLEDGEMENTS

I wish to thank Professor James Espenson for excellent mentorship throughout my graduate career. I am also thankful to the members of my research group and especially to Dr. Andreja Bakac for invaluable scientific discussions and help.

I want to particularly acknowledge my wife, Elena, for being there for me when I needed it the most and for all the help and care she provided for me.

This work was performed at Ames Laboratory for the U.S. Department of Energy. The financial support was provided by the National Science Foundation (grant CHE-9007283).

IMAGE EVALUATION TEST TARGET (QA-3)



APPLIED IMAGE, Inc
1653 East Main Street
Rochester, NY 14609 USA
Phone: 716/482-0300
Fax: 716/288-5989

© 1993, Applied Image, Inc., All Rights Reserved